

ACCEPTED MANUSCRIPT • OPEN ACCESS

A critical review on polyvinylidene fluoride (PVDF)/zinc oxide (ZnO) based piezoelectric and triboelectric nanogenerators

To cite this article before publication: Chirantan Shee *et al* 2024 *J. Phys. Energy* in press <https://doi.org/10.1088/2515-7655/ad405b>

Manuscript version: Accepted Manuscript

Accepted Manuscript is “the version of the article accepted for publication including all changes made as a result of the peer review process, and which may also include the addition to the article by IOP Publishing of a header, an article ID, a cover sheet and/or an ‘Accepted Manuscript’ watermark, but excluding any other editing, typesetting or other changes made by IOP Publishing and/or its licensors”

This Accepted Manuscript is © 2024 The Author(s). Published by IOP Publishing Ltd.



As the Version of Record of this article is going to be / has been published on a gold open access basis under a CC BY 4.0 licence, this Accepted Manuscript is available for reuse under a CC BY 4.0 licence immediately.

Everyone is permitted to use all or part of the original content in this article, provided that they adhere to all the terms of the licence <https://creativecommons.org/licenses/by/4.0>

Although reasonable endeavours have been taken to obtain all necessary permissions from third parties to include their copyrighted content within this article, their full citation and copyright line may not be present in this Accepted Manuscript version. Before using any content from this article, please refer to the Version of Record on IOPscience once published for full citation and copyright details, as permissions may be required. All third party content is fully copyright protected and is not published on a gold open access basis under a CC BY licence, unless that is specifically stated in the figure caption in the Version of Record.

View the [article online](#) for updates and enhancements.

A Critical Review on Polyvinylidene Fluoride (PVDF)/Zinc Oxide (ZnO) Based Piezoelectric and Triboelectric Nanogenerators

Chirantan Shee¹, Swagata Banerjee¹, Satyaranjan Bairagi^{2#}, Aiswarya Baburaj³, Naveen Kumar S
K³, Akshaya Kumar Aliyana⁴, Daniel M Mulvihill^{2#}, R. Alagirusamy^{1#} and S. Wazed Ali^{1#}

¹Department of Textile and Fibre Engineering, Indian Institute of Technology Delhi, Hauz Khas, New
Delhi-110016, India

²Materials and Manufacturing Research Group, James Watt School of Engineering, University of Glasgow,
Glasgow, G12 8QQ, UK

³Department of Electronics, Mangalore University, Mangalore, India

⁴Research Institute for Flexible Materials, School of Textiles and Design, Heriot-Watt University, UK

Abstract

In the recent era of energy crisis, piezoelectric and triboelectric effects are emerging as promising technologies for energy harvesting. Poly(vinylidene fluoride) (PVDF) and its copolymers are well known piezoelectric materials with high piezoelectric coefficients which are used widely in flexible electronic devices. PVDF is greatly utilized in preparation of triboelectric layer also due to its higher electronegative nature amongst common polymers. On the other hand, zinc oxide (ZnO) has been studied widely to investigate its multifunctional properties including piezoelectricity, pyroelectricity and antibacterial activity. This versatile material can be prepared, using low cost and environmental friendly routes, in various morphologies. Various research is already performed to capture the synergistic effect of reinforcing ZnO within PVDF polymeric matrix. This work firstly describes the basic principles of piezoelectric and triboelectric effects. Thereafter, piezoelectric and triboelectric performances of PVDF and ZnO based materials are briefly depicted based on their structures. Finally, challenges and future scopes, associated with the mechanical energy harvesting from such materials, are highlighted.

#Corresponding emails: wazed@iitd.ac.in; Daniel.Mulvihill@glasgow.ac.uk;
rasamy@iitd.ac.in; Satyaranjan.Bairagi@glasgow.ac.uk

1. Introduction

Sensors and smart devices have now become a customary in our day to day lives. These gadgets are a gift of the scientific innovation and progress of the recent era. As we witness the fruits of such innovations, we cannot deny the enormous energy demand accompanying them. Most of the energy requirements are met from the non-renewable fossil fuel-based energy sources. This puts tremendous pressure on the limited reserves of these energy sources, in order to meet the energy demands. [1]. As the situation is becoming alarming with time, there is a need to explore alternative sources of energy. Several non-conventional energy harvesting sources have come up in this regard. The most common green source of energy, with abundant availability is based on the ambient energy sources. Solar energy, wind energy [2,3], water energy, tidal energy, etc. have come up as promising energy sources. Undeniably, these sources of energy generate appreciable amount of power, however, their dependence on environmental factors affect their efficient functioning.

The abundant mechanical energy available around us has piqued the interest of scientific community to scavenge energy from these sources. Triboelectric [4–6] and piezoelectric [7–9] energy harvesting technologies have gained prominence as mechanical energy harvesting techniques. Further, the power generation capability, facile technologies, and scope for material development provide immense opportunity for research and innovation in this field. Triboelectricity is driven by contact electrification, while piezoelectricity is a pressure driven phenomenon. When two surfaces with different electron affinities, undergo repeated contact and separation cycles, they generate surface charges of opposite polarity on their respective surfaces. This phenomenon is referred as contact electrification [10–12]. It is the driving factor behind the triboelectric effect. Piezoelectricity, on the other hand, is a material property. The application of force on piezoelectric materials leads to disturbance in their crystal structure, which causes a potential difference between its surfaces. This potential difference can be harvested in the form of electric energy to power electronic gadgets. This illustrates the direct piezoelectric effect. The dimensional changes of a

1
2
3 piezoelectric material as a response to applied electric field is called the converse
4 piezoelectric effect [13]. Piezoelectric materials can be classified as: single crystals,
5 polymers, ceramics, and composites [14–18]. Each of these category of materials have
6 unique characteristics that are explored in a wide variety of applications. Composites
7 comprise of one or more constituents, where each element has exclusive properties. The
8 property of the composite is distinct from its constituent elements. They improve upon the
9 advantages of each constituent while overcoming their drawbacks.

10
11 Poly(vinylidene fluoride) (PVDF) is one of the most explored piezoelectric polymers. The
12 appreciable piezoelectric coefficients of this polymer make it suitable for a wide range of
13 applications. The polar nature of this polymer is due to the presence of CF_2 dipole. PVDF
14 exist in more than one crystalline phases, namely α , β , γ , etc. All the phases do not show
15 piezoelectric character. This is due to the difference in the polymer chain conformations in
16 each phase. The β phase of PVDF with all-trans conformation is the desirable electroactive
17 phase of the polymer [13]. There are several ways of achieving and stabilizing this phase of
18 PVDF. Techniques like electrospinning, result in in-situ poling of the polymer chains,
19 resulting in enhanced piezoelectric activity [19,20]. Piezoelectric composites of PVDF with
20 different incorporated fillers[21–23] have also been explored to produce advanced
21 composites with appreciable properties [24][25][26].

22
23 Zinc oxide (ZnO) is a popular semiconducting material. This material has multifunctional
24 properties that are explored in areas like piezoelectricity, anti-bacterial activity, UV
25 protection, to name a few. ZnO can be easily synthesized in various morphological
26 structures. Apart from piezoelectricity, ZnO is also used for mechanical energy harvesting
27 with triboelectric effect due to its positive triboelectric charge density.

28
29 Extensive research has been carried out to explore the piezoelectric performance of
30 PVDF/ZnO composite. Electrospun mats, solution cast films and several other techniques
31 have been explored for preparation of PVDF/ZnO piezoelectric composites. Electroactive
32 phase of PVDF can be improved by several means and piezoelectric ZnO can be synthesized
33 in a relatively easy fashion to obtain various nanostructures. This promising piezoelectric
34 combination has been used in different forms for a variety of applications. Though there is
35 extensive literature on composite of PVDF/ZnO, a conclusive review compiling the
36
37
38
39
40
41
42
43
44
45
46
47
48
49
50
51
52
53
54
55
56
57
58
59
60

different methodologies for the composite preparation, their respective properties and application seems to be scanty. This review provides a conclusive report on PVDF/ZnO piezoelectric composites fabricated through different techniques and their properties reported thereof.

2. Mechanical energy harvesting

2.1 Piezoelectricity

Piezoelectricity is a stress-induced phenomenon that helps to convert mechanical energy into electrical energy and vice versa. The word piezoelectricity has been derived from the Greek word “piezein” which means to squeeze or press. When any piezoelectric material is subjected to stress, it undergoes a distortion in its crystalline structure. This causes a local charge imbalance in the unit crystals leading to the creation of potential difference between its surfaces (**Fig. 1**). This potential difference can be harvested in the form of electrical energy. This phenomenon is called the direct piezoelectric effect. Interestingly, this effect is reversible in nature. When a piezoelectric material is subjected to electric field, it causes a geometric strain in its structure. This is called the converse piezoelectric effect. This phenomenon can be illustrated mathematically in the form of following equations [13]:

$$P = d \times T \dots \dots \dots \text{for direct piezoelectric effect (i)}$$

where P is polarization, d is piezoelectric strain coefficient and T is the applied stress.

$$S = d \times E \dots \dots \dots \text{for converse piezoelectric effect (ii)}$$

where S is mechanical strain and E is the applied electric field.

These equations can further be reconstructed into linear constitutive equations as follows:

$$S_p = s_{pq}^E T_q + d_{pk} E_k \dots \dots \dots \text{(iii)}$$

$$D_i = d_{iq} T_q + \varepsilon_{ik}^T E_k \dots \dots \dots \text{(iv)}$$

s_{pq}^E is elastic compliance tensor at constant electric field, d_{pk} is piezoelectric constant tensor, T_q is mechanical stress in q direction, ε_{ik}^T is dielectric constant tensor under constant

stress, E_k is the electric field in k direction, D_i is electric displacement in i direction and S_p is the mechanical strain in p direction.

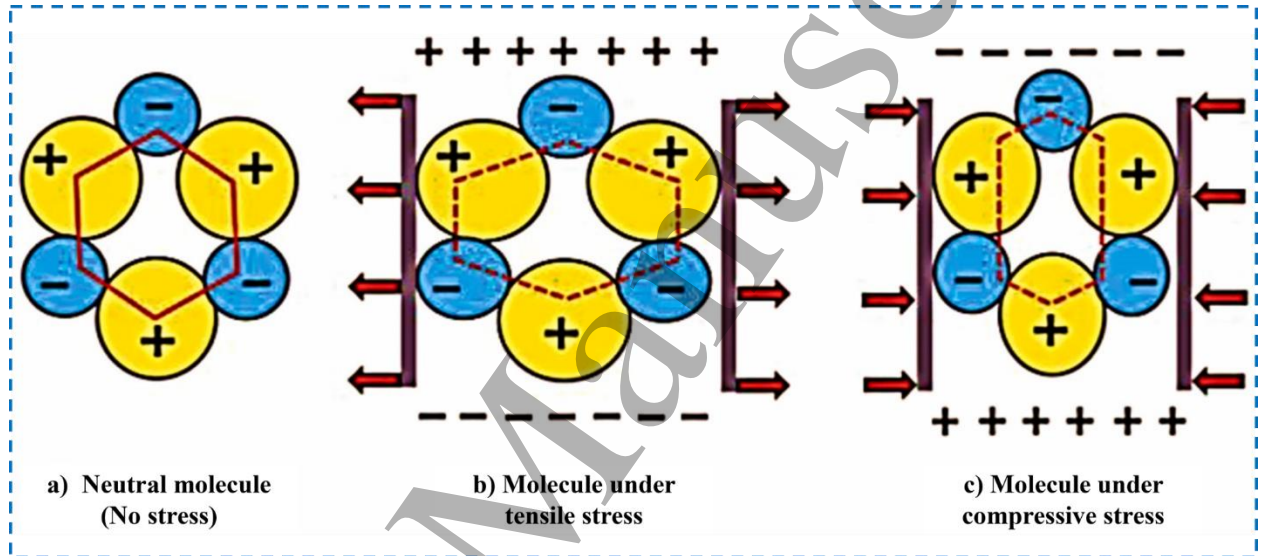


Fig. 1. Schematic representation of crystal structure distortion of piezoelectric materials under stress [13] All essential copyrights and permissions taken.

Piezoelectric materials are classified broadly into single crystals, ceramics, polymers and composites [27]. Each of these classes have their respective advantage and disadvantages. The piezoelectric crystals are among the first materials to show piezoelectricity. They have very good piezoelectric property, but are expensive for daily use. The piezoelectric ceramics show promising piezoelectric properties. These materials have high piezoelectric coefficients, however, they are fragile and brittle in structure. This fragility restricts their use in areas requiring flexibility. Based on chemical composition, the piezoelectric ceramics can be lead based or lead free. Owing to the established toxicity issues of lead, the preference of lead free ceramics is increasing. Numerous lead free materials are developed to serve as appropriate alternative to lead based piezoelectric ceramics [28]. Piezoelectric polymers are good candidates for sensing purposes. These materials have high voltage

1
2
3 coefficients that render them suitable for functioning as sensors. These are flexible materials
4 and finds application in flexible wearables. The piezoelectric composites are generally made
5 up of a matrix and reinforcement. The matrix is usually a piezoelectric polymer, while the
6 filler materials is a piezoelectric ceramic. The composite thus formed has properties distinct
7 of its constituent elements. It helps to make a flexible material with appreciable
8 piezoelectric coefficients. Thus, based on target application, the piezoelectric material can
9 be synthesized and modified. This provides a wide space for material development and
10 novel applications [29].
11
12
13
14
15
16
17
18
19

20 **2.2 Triboelectricity**

21
22 Triboelectric nanogenerators (TENGs) are cutting-edge devices that collect energy from
23 mechanical motion, largely via the triboelectric effect [30]. These devices have received a
24 lot of interest in recent years because of their ability to transform ambient and human-
25 generated mechanical energy into useful electrical power [31]. TENGs have emerged as a
26 potential technology for a variety of applications, including self-powered electronics, sensor
27 networks, and wearable devices, due to their ability to capture energy in a sustainable and
28 efficient manner. The triboelectric effect and electrostatic induction are at the root of a
29 TENG's operation [32]. TENGs are often made up of two materials in contact with each
30 other, one having a high electron affinity and the other with a low electron affinity [33,34].
31 When these materials are rubbed together or mechanically deformed, electrons transfer
32 between them, resulting in a transient charge imbalance [35,36]. The material with the
33 greater electron affinity is negatively charged, while the other material is positively charged
34 (**Fig. 2**). This charge separation generates an electric potential between the two materials.
35 TENGs employ a structured design with electrodes and an external load to harness this
36 electric potential and generate usable electrical current [37,38]. The potential difference
37 between the two triboelectric materials causes the flow of electrons, providing an electric
38 current that can be caught by the electrodes and sent to an external circuit as the two
39 triboelectric materials are separated and brought back into contact through mechanical
40 motion. TENGs can create a continuous and renewable source of electrical power due to the
41 continual cycle of separation and contact caused by mechanical motion or vibration [39,40].
42
43
44
45
46
47
48
49
50
51
52
53
54
55
56
57
58
59
60

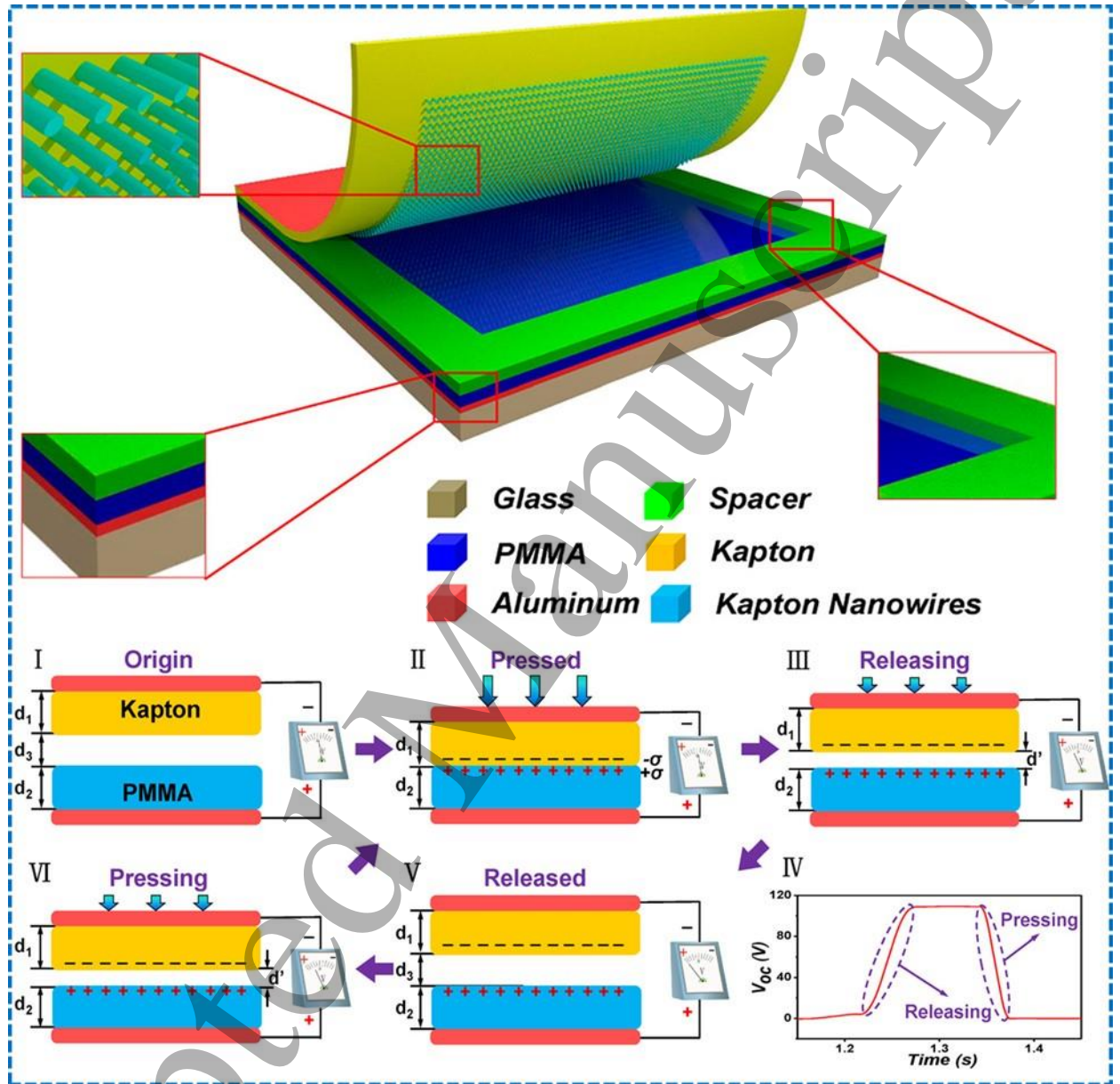


Fig. 2. Schematic illustrations of the TENGs structure and materials selection showing the operating principle of the TENGs in contact-separation mode [41]. Reprinted (adapted) with permission from (Nano Lett. 2012, 12, 9, 4960-4965). Copyright (2023) American Chemical Society.

1
2
3 The triboelectric series comprises a hierarchical classification of materials based on their
4 proclivity to gain or lose electrons when they come into contact with one another. Materials
5 near the bottom of this series, such as Teflon (polytetrafluoroethylene or PTFE)[42,43],
6 have a tendency to become negatively charged during contact, whereas metals and other
7 materials at the top tend to acquire a positive charge during contact. In the context of
8 TENGs, this hierarchical classification is critical since it regulates the degree of electron
9 transfer during triboelectric interactions. It is advantageous to use materials with a
10 significant variance in their ranks within the triboelectric series to optimize power
11 generation in a TENG [44,45]. Materials with a wide range of triboelectric properties are
12 desirable in situations where human motion, such as walking or finger tapping, serves as
13 the energy source. Materials that closely align in the triboelectric series, on the other hand,
14 can be selected to assure stable and continuous power output in applications involving
15 continuous mechanical motion or high-frequency vibrations. As a result, rigorous
16 examination of the triboelectric series is required to fine-tune the performance and
17 efficiency of TENGs in a variety of applications[46,47]. TENGs operate on a set of
18 fundamental equations that govern their energy generation process [48,49].

19
20
21
22
23
24
25
26
27
28
29
30
31 They generate electric charge through the triboelectric effect, where two materials come
32 into contact and then separate. This charge separation leads to the production of electric
33 charge, which is represented by the equation, $Q = C \times \Delta V$. Q denotes the electric charge
34 produced, C signifies the effective capacitance of the TENG, and ΔV accounts for the
35 voltage generated due to the charge separation between the materials.

36
37
38
39
40
41 The voltage generation in TENGs is determined by the difference in work functions (Φ)
42 between the materials involved. This voltage is captured by the equation $\Delta V = \Phi_1 - \Phi_2$,
43 where ΔV represents the voltage output. The resulting voltage potential is a direct
44 consequence of the work function disparity between the two materials, creating an electric
45 potential.

46
47
48
49
50 The current produced by TENGs follows Ohm's law, which is expressed as $I = \Delta V / R$. In
51 this equation, I represents the current generated, ΔV stands for the voltage produced, and R
52 is the external load resistance in the electrical circuit. This equation highlights the dynamic
53
54
55
56
57
58
59
60

1
2
3 control over the current by adjusting the external load resistance to meet specific power
4 requirements [48,50,51].
5

6
7 The choice between these equations depends on whether optimization for high current or
8 high voltage output is desired, aligning the TENG's performance with the unique demands
9 of the application at hand. These equations form the core of TENG operation, enabling them
10 to effectively harness mechanical energy for power generation. TENGs can be integrated
11 into a wide range of applications and surroundings that have readily available mechanical
12 energy, including footfall [52,53], wind [54], and even minor vibrations [52,53]. Because
13 of their ability to generate power from small, intermittent mechanical inputs, they are perfect
14 for powering low-energy devices and sensors, decreasing reliance on traditional batteries
15 and encouraging sustainable energy solutions. TENGs are also low-cost and eco-friendly,
16 making them a potential technology for the future of energy harvesting and self-sustaining
17 systems.
18
19
20
21
22
23
24
25

26 27 **3. Piezoelectric and triboelectric materials**

28 A material should have some unique properties in order to show piezoelectricity. Non-
29 centrosymmetry in crystal structure is essential for exhibiting piezoelectric property.
30 Piezoelectric materials can be broadly classified as single crystals, ceramics, polymers and
31 composites. According to the symmetry, single crystals can be divided into 32 groups,
32 amongst which only 21 are non-centrosymmetric in nature. Within these non-
33 centrosymmetric crystal structures, only 20 can show piezoelectric effect. The exceptional
34 group is non-piezoelectric due to other symmetry elements. Although single crystals have
35 higher mechanical quality factor but costly and complex processing techniques deteriorates
36 their popularity to some extent. Quartz crystal and ammonium dihydrogen phosphate are
37 the examples of piezoelectric crystals. Talking about piezoelectric ceramics, they have
38 higher sensitivity, coupling factor, dielectric constant and good chemical stability. On the
39 contrary, brittleness, high density, costly processing techniques and small strains are well
40 known limitations of piezoelectric ceramics. Barium titanate (BaTiO_3), ZnO, Lithium
41 niobate (LiNbO_3), Potassium niobate (KNbO_3), Gallium nitride (GaN) are few examples of
42 piezoelectric ceramics. Unlike piezoelectric ceramics, where crystal structure
43 predominantly determines the piezoelectricity, the piezoelectric polymers show
44
45
46
47
48
49
50
51
52
53
54
55
56
57
58
59
60

piezoelectric property as a result of attraction and repulsion of entangled polymeric chains. Despite inferior electromechanical coupling, piezoelectric polymers are primarily suitable for wearable electronics applications due to their higher flexibility, easy processing technique, lead-free structure, lower cost and lower density. Typical examples of piezoelectric polymers are PVDF, nylon11 and PAN. So, at this point it is clear that each class of piezoelectric material has its own advantages and limitations. In order to realize the benefits of different classes along with suppressing their disadvantages, often piezoelectric composites are manufactured by combining filler materials and polymeric matrix in which at least one phase is piezoelectric in nature. Synergistic effect of each constituent can be effectively achieved in this class of piezoelectric materials, but neutralization of dipoles is possible due to inconsistent polarization direction. (BaTiO₃+PVDF), (PbTiO₃+PVDF) are few examples of this class [55,56]. Various forms of ZnO are also being used to be added into PVDF matrix, which will be thoroughly discussed in the subsequent sections. The triboelectrification process depends on physical and chemical nature of the two surfaces, environmental factors and physical mode of contact-separation cycle. That is why even after millennia of its discovery, the involved mechanism in it, is not clear till now [57]. Triboelectric series, as discussed earlier, is purely empirical in nature. Contact electrification experiments have been done followed by measuring the polarities of the materials as a result of contact-separation cycle. Polarity of the charged surfaces and amount of charge are two independent phenomena. Generally, it is assumed that far is the gap between the two materials, higher will be the charge produced. Zhang et al. stated that the triboelectric charge transfer is based on the lewis basicity of the material [58]. Numerous materials have been already well explored experimentally in order to assess their triboelectric performance. In this context, PVDF as a polymer and ZnO as a metal oxide perform very well as triboelectric materials. Triboelectric charge density for PVDF is negative whereas the same for ZnO is positive [59,60]. This is another reason for making these two multifunctional materials good choices for triboelectric materials.

PVDF: PVDF, polymer of difluoroethylene, is known to have maximum piezoelectric property amongst the common piezoelectric polymers. CF₂ bond, within PVDF, exhibits strong dipole moment of 7×10^{-30} C.m. PVDF shows different phases, namely α , β and γ depending on their polymeric structure (**Fig. 3(a)**). Although α -phase is thermodynamically

1
2
3 stable, it is non-polar in nature due to the alternating trans(T)-gauche(G) conformation,
4 resulting in zero net dipole moment. β and γ phases of PVDF are polar in nature due to the
5 TTTT and TTTGTTTG [61,62] conformations of polymer chains. There are few more
6 crystalline forms of PVDF, however they have not gained much popularity in this aspect
7 [63]. β phase of PVDF has high dipole density due to opposite arrangement of fluorine and
8 hydrogen atoms along the carbon chain. This phase thus produces a high dielectric constant
9 value of 10 [64]. Therefore, this phase is regarded as the desirable electroactive phase of
10 PVDF. It is utilized in piezoelectric energy harvesting. Most of the PVDF polymer-based
11 composites aim at enhancing this electroactive phase content to improve the piezoelectric
12 performance of the composite. In case of triboelectric effect, the β phase helps in
13 accumulation of charge at the solid interface that helps in enhancing the performance of
14 triboelectric nanogenerators [65]. The presence of fluorine based functional groups in
15 polymer chain helps to improve the charge accepting nature of the polymer, during the
16 contact electrification phenomenon [66]. Hence, PVDF has been modified to produce
17 PVDF-copolymers with different fluorine containing groups. The inclusion of bulky
18 fluorine functional groups increases the interchain distance, thus weakening the dipole
19 interaction. This results in relaxor ferroelectric properties of the polymer. Such polymers
20 align their dipole in the direction of applied electric field. However, due to weak dipole-
21 dipole interaction, the alignment is disturbed once the electric field is removed. This gives
22 rise to good dielectric constant values with inferior piezoelectric polarization. Such
23 characteristics affect the piezoelectric and triboelectric properties of the material [67]. The
24 α -phase of PVDF can be transformed to electroactive β -phase with the help of high
25 temperature annealing treatment or mechanical stretching. Electrical poling also improves
26 the piezoelectric property. Piezoelectric polymers require 30-120 kV/mm electric field
27 strength for poling whereas 3 kV/mm field is sufficient for ceramic materials. Apart from
28 the dipole moment, crystallinity of a polymeric material also determines the piezoelectricity.
29 In a typical polymeric material, the crystallinity can reach as high as 50%. PVDF is often
30 used as a copolymer of trifluoroethylene. This material can offer crystallinity up to 90%
31 improving piezoelectric property as well as operating temperature of the polymeric system
32 [55].
33
34
35
36
37
38
39
40
41
42
43
44
45
46
47
48
49
50
51
52
53
54
55
56
57
58
59
60

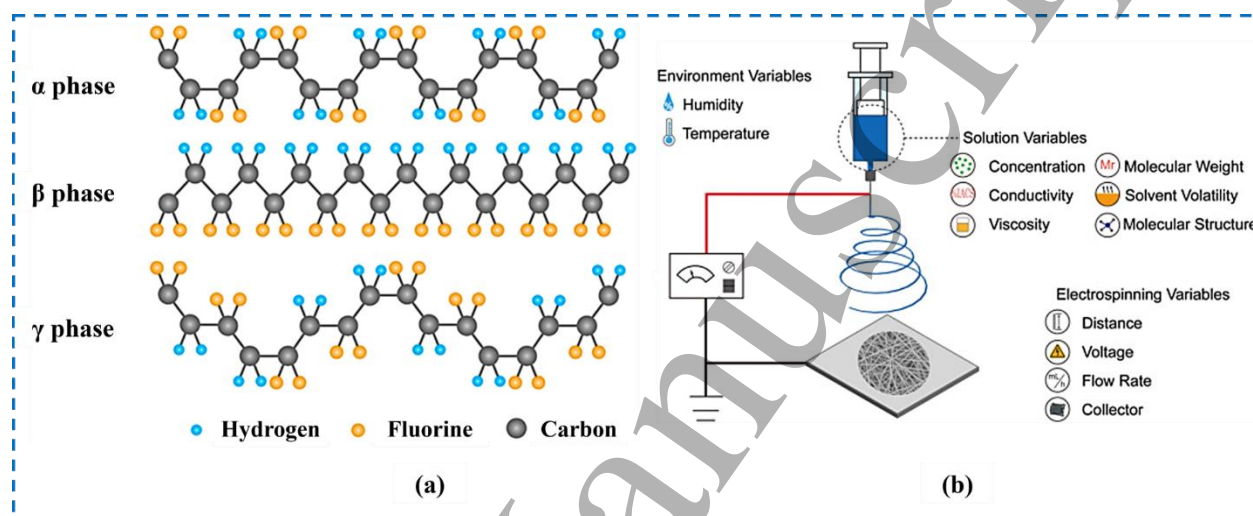


Fig. 3 (a). Crystalline phases of PVDF [68] **(b)** Schematic representation of electrospinning technique [69] All essential copyrights and permissions taken.

Content of different crystalline phases can be quantified using Fourier Transform Infrared (FTIR) Spectroscopy and X-Ray Diffraction (XRD) analyses. In FTIR spectra of PVDF, peaks corresponding to 1280 and 840 cm^{-1} represent the presence of β -crystalline phase whereas peaks corresponding to 1182, 1073, 878, 765 cm^{-1} confirms the presence of α -phase. Using the following equation, the fraction of β -phase can be calculated. In this equation, A_{β} and A_{α} are the absorbance values at the wavenumbers of 841 and 765 cm^{-1} , respectively.

$$F(\beta) = \frac{A_{\beta}}{1.26A_{\alpha} + A_{\beta}}$$

XRD results also exhibit the signatures of α and β -phases. Peak corresponding to $2\theta = 20.8^{\circ}$ can be assigned to β -phase of PVDF. Moreover, three peaks at $2\theta = 18.4^{\circ}$, $2\theta = 26.6^{\circ}$ and $2\theta = 35.7^{\circ}$ can be attributed to the α -phase of PVDF. $2\theta = 20.1^{\circ}$ can be assigned to γ -phase

of PVDF [70]. In addition to FTIR and XRD, differential scanning calorimetry (DSC) is another technique for identification of different crystalline phases of PVDF. However, each technique has its own benefits and limitations. In FTIR spectra, α -phase can be easily distinguishable whereas the peaks for β -phase and γ -phase are similar. On the other hand, XRD diffraction peaks for α -phase and γ -phase are superimposed on each other simultaneously providing identifiable peak for β -phase. Additionally, DSC can clearly identify the presence of γ -phase of PVDF. So, more than one technique can offer vivid identification and quantification of different crystalline phases of PVDF [71].

Electrospinning process has the potential to increase the β -phase content of PVDF due to in-situ stretching and poling of polymeric chains. Jiyong et al. studied the effect of electrospinning parameters like applied voltage, flow rate and needle diameter on the content of β -phase. They have observed that with increasing applied voltage, the β -phase content firstly enhances followed by decreasing trend. Applied voltage of 14-24 kV is found to be beneficial for formation of electroactive β -phase. Increase in β -phase with enhancement in applied voltage can be attributed to the improved dipolar alignment and mechanical stretching during electrospinning process. However, further increase in applied voltage hampers the jet stability and reduces the traveling time of the jet ultimately causing an increase in α -phase content. Generally, content of β -phase decreases with increase in flow rate of the polymer solution and increase in needle diameter [70].

ZnO: ZnO is a wide band-gap semiconductor which finds extensive use in various industrial sectors. Apart from the obvious properties of ZnO due to its chemical constitution, the wurtzite structure of ZnO imparts piezoelectric characteristic to it. The structure is devoid of a centre of symmetry and has a polar nature along [001] crystallographic direction. This influences the piezoelectric nature of ZnO. However, no ferroelectric switching has been observed for this semiconductor material. The structure of ZnO can be illustrated as alternative arrangement of planes, comprising of tetrahedrally coordinated Zn^{2+} and O^{2-} ions along the c-axis. The crystallographic arrangement of anions and cations in a specific manner leads to the generation of polar surfaces. This charge dominated surfaces may result in some topological variations that in turn lead to improvement in properties of ZnO. Under neutral conditions, the centres of the positive and negative charges coincide with each other.

When subjected to stress along c-axis, these centres deviate away from each other forming dipole moment in the crystal [72–74]. ZnO nanostructures of various dimensions can be synthesized through a variety of routes [75]. The numerous synthesis techniques, high piezoelectric coefficients, multifunctional properties of ZnO have escalated the research in the material [76].

4. PVDF/ZnO composite based nanogenerators (NGs)

4.1 PVDF/ZnO composite based piezoelectric nanogenerators (PENGs)

4.1.1 Electrospun membranes based PENGs

Electrospinning is a technique of micro/nano fibre manufacturing with the help of application of electric field (**Fig. 3(b)**). Firstly, the polymer solution is loaded into a syringe. Next the solution is forced to exit from the needle tip of the syringe to ultimately form a droplet. Thereafter, external electrical voltage is applied to the needle, so that electrical charges accumulate within the polymer solution. When the electrostatic repulsion exceeds the surface tension and viscoelasticity of the solution, the droplet assumes a shape of cone and finally stretched to form fibres. Concentration of the polymer solution is a determining factor of charged jet stability. If the concentration is sufficient to maintain the stability of the jet, the elongation of the droplet happens remarkably ultimately forming nonwoven meshes, consisting of fibres, on the grounded collector. However, low concentration of the solution destabilizes the charged jet which results in small spherical particles after evaporation of the solvent. This is known as electrospraying. Costa et al. reported the critical concentration of PVDF solution for electrospraying to electrospinning transition for different solvents [77].

Kim and Fan studied the effect of different structural combinations on the piezoelectric property of nanofibrous composites. Three combinations were considered for this study as follows: (i) electrospinning solution was prepared using pre-synthesized ZnO nanorods (NRs) and PVDF followed by electrospinning the composite solution to obtain nanocomposite fibrous membrane (ZnO+PVDF), (ii) ZnO NRs were grown onto electrospun PVDF membrane to obtain (ZnO@PVDF), (iii) ZnO NRs were dispersed into water followed by electrospraying the solution onto PVDF electrospun membrane to get

(ZnO/PVDF) structure. It was found that for all the cases the electroactive β -phase of PVDF decreases with addition of ZnO NRs. The maximum decrement was observed for (ZnO/PVDF) structure. While electrospinning ZnO NR dispersion, the electric field was being applied onto the pristine PVDF membrane in the thickness direction. Initially after the electrospinning of pristine PVDF, the dipoles were oriented in fibre axis direction. Afterwards during electrospinning ZnO NR dispersion, the orientation of the dipoles gets disturbed ultimately resulting in lower β -phase. Although it can be expected that the resultant dipole orientation would be in the direction of fibre axis as electric field during electrospinning of pristine PVDF is more effective compared to the electrical poling during electrospinning ZnO dispersion at room temperature. On the other hand, decrease in β -phase content for (ZnO+PVDF) can be attributed to the less crystallization of polymer in the presence of filler at higher concentration. For ZnO@PVDF structure, the deterioration of β -fraction can be attributed to the heat relaxation of PVDF crystalline region during hydrothermal growth of ZnO NRs. Descending order of power output was found for the power outputs arising from ZnO/PVDF, ZnO@PVDF, pristine PVDF and ZnO+PVDF membranes. The reasons for the least power output of ZnO+PVDF membrane are decreasing the crystallinity of PVDF during electrospinning and increasing dielectric constant of nanocomposite structure due to addition of nanofillers. The higher power outputs for ZnO/PVDF and ZnO@PVDF can be attributed to the triboelectric charge generation. From FESEM images, it can be visually assessed that for these two structures the surface roughness is higher compared to the remaining two structures. Higher surface roughness and specific surface area lead to enhanced surface charge density improving the triboelectricity [78]. Yang et al. grown ZnO NRs onto electrospun PVDF surface to obtain hierarchically interlocked PVDF/ZnO structure with higher pressure and bending sensitivities compared to the same of pristine PVDF membrane. The mechanical durability and real-time applications of this device have been extensively investigated. The device, fabricated with such hierarchical structure, not only can monitor physiological movements but is also useful for disease diagnosis (**Fig. 4**) [79].

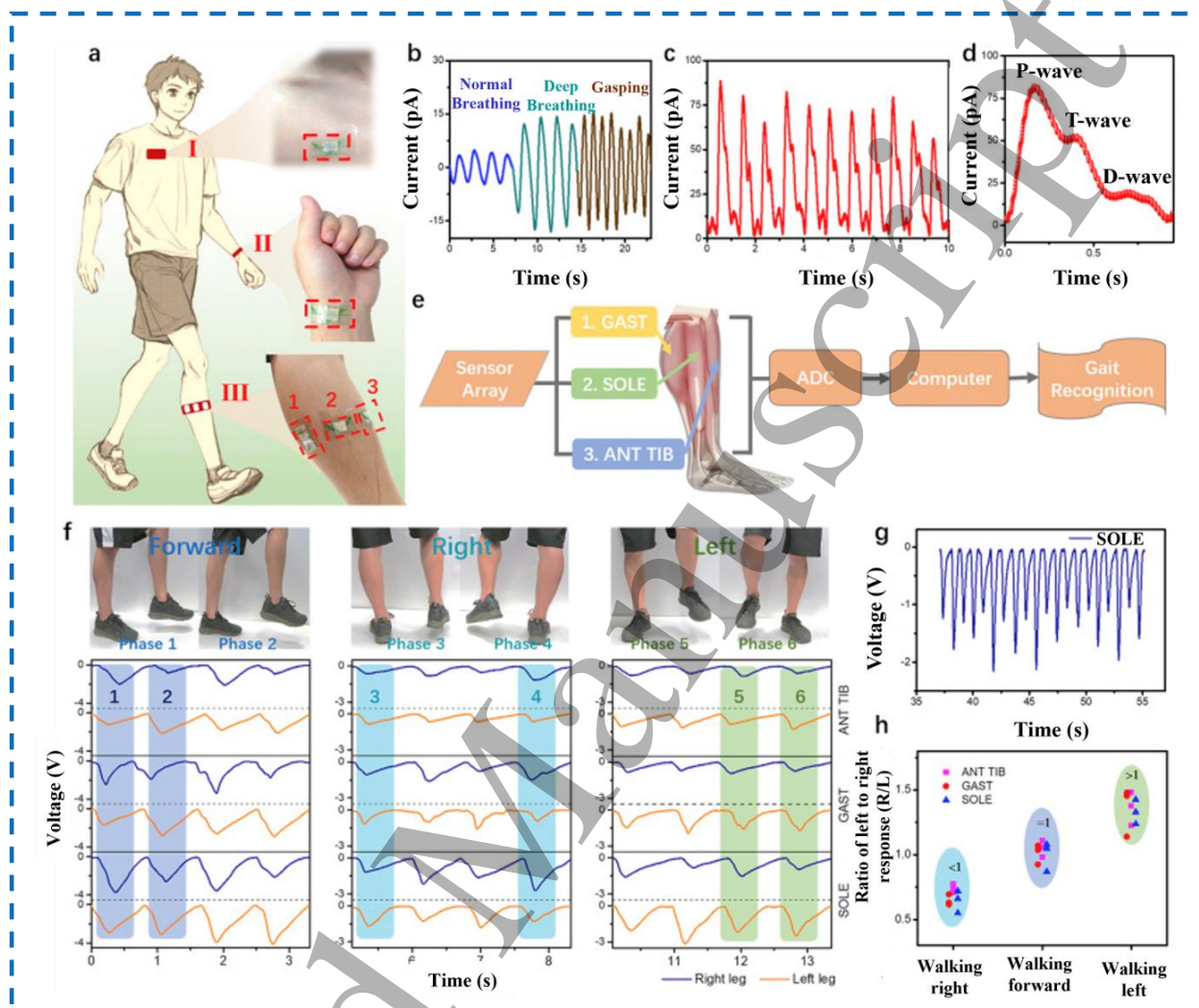


Fig. 4. (a) Pressure sensor at different body parts, (b) Electrical current generated from breathing pattern, (c) Electrical signal from wrist pulses, (d) Three peaks in an expanded pulse, (e) Representation of gait recognition system, (f) Detection of gait states during walking in different directions, (g) Multiple electrical signals for the left leg during walking in left direction, (h) Ratio of calf response amplitudes for right and left legs respectively, in different directions [79] All essential copyrights and permissions taken.

Feng et al. grown ZnO NRs onto conductive fabric followed by sandwiching PVDF in between the conductive fabric electrode and the electrode with ZnO NRs. Incorporation of ZnO layer increases the piezoelectric output voltage noticeably. Apart from piezoelectric property, this textile based breathable device offers waterproof behaviour. The device, with high sensitivity, durability and output voltage, can be utilized to monitor environmental

1
2
3 changes like wind blow and rainfall [80]. Mahanty et al. demonstrated the stress
4 concentration behaviour within PVDF/ZnO nanocomposite fibre using finite element
5 method (FEM). PVDF fibre loaded with ZnO nanoparticles (NPs) offers higher stress
6 concentration compared to PVDF loaded with ZnO nanorods (NRs). The authors depicted
7 the piezoelectric performance of PVDF/ZnO composite electrospun membrane. The ultra-
8 fast response of the device proves the potential of the same to be used in sensing
9 applications. Moreover, the device is not only capable of lightening five LEDs without any
10 electrical storage system but also can charge a capacitor of 2.2 μF after rectification of the
11 output voltage using a bridge rectifier circuit. The device is also capable of sensing several
12 physiological movements like pulses, vocal chord vibrations resulting in making the device
13 suitable for monitoring the health condition of patients [81].

22
23 Research has been executed on the effect of filler addition on the piezoelectric property of
24 electrospun PVDF membrane. Li et al. prepared carbon coated ZnO (ZnO@C) NPs
25 incorporated PVDF electrospun membranes. They have observed that with increase in
26 ZnO@C content within the nanofibrous membrane, the content of β -phase enhances within
27 PVDF which can improve the piezoelectric performance of the device, fabricated using such
28 electrospun membrane. Carbon layer contains sp^2 hybridized carbon atoms which are
29 having negative charges. On the contrary, CH_2 dipoles within PVDF are positively charged.
30 Interaction between positively charged dipoles and negatively charged carbon layer results
31 in regular arrangement of PVDF segments thus β -phase is formed. Moreover, the
32 conductive nature of carbon shell layer accumulates more electrical charges in this region
33 in the presence of an electric field. This further improves the interfacial polarization
34 ultimately leading to improvement in electroactive phase of PVDF [82]. Ongun et al.
35 incorporated ZnO NPs and Ag doped ZnO NPs within electrospun PVDF membrane. They
36 have found that electroactive β -phase of PVDF enhances with the rise in amount of ionic
37 Ag dopant. With increase in Ag dopant concentration, the capacitance of the nanocomposite
38 device also enhances [83]. Deng et al. prepared ZnO nanosphere incorporated PVDF
39 electrospun fibrous membrane with cowpea structure. It was found that electroactive β -
40 phase of PVDF increases as a result of ZnO addition within the fibrous structure. The sensor
41 was fabricated by spraying Mxene dispersion onto the electrospun membrane followed by
42 extracting the electrode using copper wire. With the increase in the applied force the open-
43
44
45
46
47
48
49
50
51
52
53
54
55
56
57
58
59
60

1
2
3 circuit voltage and short-circuit current have a tendency to rise. As prepared piezoelectric
4 sensor can function under both the pressing and bending excitations without any external
5 power source. The sensor not only exhibits high sensitivity and good flexibility but also can
6 help in remotely control of the robot hand proving its application in interactive human-
7 machine interface (**Fig. 5**) [84]. Often, addition of conductive filler and piezoelectric filler
8 to polymer matrix, has been carried out to explore their synergistic effect on stabilizing the
9 electroactive phase of the polymer. Carbon nanotube is a widely used conductive filler in
10 piezoelectric composites. The homogeneous dispersion of these fillers has a considerable
11 effect on the piezoelectric performance of the composites. Single walled carbon nanotubes
12 were decorated with ZnO through a wet chemical route and incorporated into electrospun
13 PVDF nanofibrous web. The inclusion of this surface decorated carbon nanotubes into
14 PVDF promoted its β phase formation(95%) and improved its thermal stability and tensile
15 properties. The nanogenerators produced an output voltage of 15.5V and power density of
16 $8.1\mu\text{W}/\text{cm}^2$ [85]. The performance of PVDF/ZnO electrospun composite can be influenced
17 by the shapes and content of the filler. Nanosticks and nanorods have proved to perform
18 better as piezoelectric reinforcement in an electrospun nanocomposite [86]. Studies on
19 piezoelectric films made from PVDF/ZnO nanoparticles further ascertained the ability of
20 ZnO nanoparticles to promote the β phase formation of PVDF polymer. ZnO nanoparticles
21 lower the transition energy from α to β phase of PVDF, thus improving its electroactive
22 phase content. This effect is more pronounced at lower levels of ZnO nanoparticle addition.
23 At higher levels, however, these nanoparticles halts the polymer chains, that adversely
24 affects the crystallisation process. Thus, the overall crystallinity decreases at higher filler
25 loadings. The morphological studies of the composite cross-section, further confirms the
26 compatibility of the nanoparticles with the polymer matrix. The optimized composition of
27 the composite yielded an open circuit voltage of 69V under an impact force of 1.6N. it also
28 generated an appreciable surface power density of $250\mu\text{W}/\text{cm}^2$ [87]. Simulation studies on
29 PVDF/ZnO piezoelectric composite explains the improved performance of the composite
30 compared to pristine material. It was observed that enhanced distribution of stress at the
31 interface of filler and matrix increased the Young's modulus and piezoelectric coefficient.
32 These effects lead to an enhanced piezoelectric performance of the composite in comparison
33 to pristine polymer [88].
34
35
36
37
38
39
40
41
42
43
44
45
46
47
48
49
50
51
52
53
54
55
56
57
58
59
60

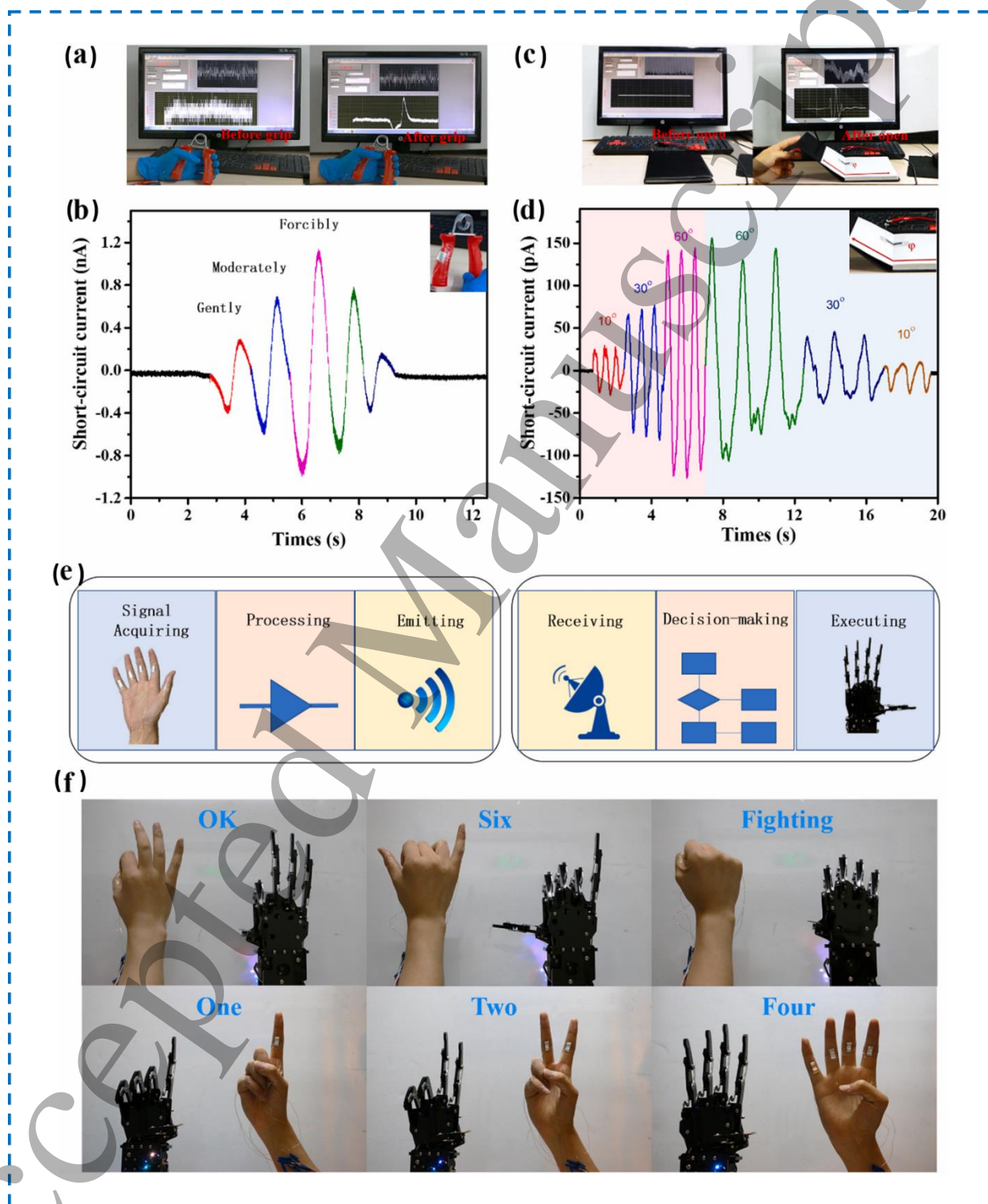


Fig. 5. (a) Detecting the power of gripping of a spring-grip, (b) Electrical outputs for various grip strength, (c) Detection of the angle of opening and closing book, (d) Electrical outputs

1
2
3 for closing (red area) and opening (blue area) of a book, (e) Schematic representation of
4 human-machine remote control system, (f) Application of gesture remote control [84] All
5 essential copyrights and permissions taken.
6
7

8
9 Yi et al. synthesized Y-doped ZnO followed by incorporation of the same into PVDF with
10 the help of electrospinning technique. Y-ZnO incorporated electrospun membrane offered
11 superior piezoelectric output voltage compared to the ZnO incorporated membrane due to
12 higher polar face in the former filler. It was also observed that with increasing the
13 electrospinning time, the piezoelectric output enhances. Corona poling was found to be an
14 efficient technique to improve the piezoelectricity of porous material through dipolar
15 electret formation. Porous electrospun membrane exhibited lower piezoelectricity
16 compared to the same of aligned electrospun membrane while the trend reverses after
17 corona poling treatment as a result of higher electret dipoles formation within porous
18 structure. The device fabricated using Y-ZnO incorporated PVDF membrane was able to
19 charge capacitors of various capacitance values. Additionally, it was tested for producing
20 piezoelectric output voltage from the biomechanical motions like walking and running [89].
21
22
23
24
25
26
27
28
29

30 **4.1.2 Textile based materials**

31
32 The growing field of electronic wearables has led to the expansion of textiles from
33 conventional uses to high performance applications. The flexibility, conformability,
34 comfort, and aesthetic appeal of textiles have made it the appropriate substrate for such
35 applications. Textiles in the form of woven or knitted structures are being explored widely
36 for such electronic wearable applications. Piezoelectric grade fibres produced through
37 different processes are shaped in the form of textile structures and used for harvesting
38 energy from mechanical sources [90].
39
40
41
42
43
44

45 Melt spinning is one of the widely used processes for preparation of piezoelectric fibres.
46 There are several studies that illustrate the fabrication and use of melt spun piezoelectric
47 fibres. In a study, core sheath PVDF based melt spun filaments were produced. The core
48 consisted of carbon black/high density polyethylene acting as inner electrode, while the
49 sheath was made up of electroactive PVDF. These core sheath piezoelectric PVDF filaments
50 produced a piezoelectric signal with peak-to-peak voltage amounting to 40 mV when
51 subjected to compression. Such electrode embedded piezoelectric PVDF filaments can be
52
53
54
55
56
57
58
59
60

1
2
3 explored as single fibre sensors [91]. Further, studies have shown that poling of such
4 filaments under appropriate temperature and electric field conditions improve their
5 piezoelectric properties. These filaments when shaped in the form of woven textiles, were
6 suitable to monitor the heartbeat of humans [92,93]. Melt extruded PVDF fibres and flexible
7 electrodes were introduced into polyester plain woven fabric, to prepare a flexible textile
8 based sensor. The signals produced by this sensor were different for different force
9 waveforms. The distance between the electrodes was tailored by varying the number of
10 spacer yarns between them. This noticeably influenced the output of the sensor [94].
11 Sometime, porous PVDF fibres are also produced through processes like wet spinning to be
12 utilized in filtration application. This porosity can be tuned by varying the drawing ratios
13 and temperatures in the subsequent drawing baths [95].
14
15
16
17
18
19
20
21
22

23 ZnO has been used extensively in the textile industry owing to its properties like ultraviolet
24 resistance, anti-fungal activity, piezoelectric characteristics, etc [96]. ZnO nanorods were
25 grown on cotton substrate using low temperature chemical synthesis method. The cotton
26 substrate was coated with silver to facilitate the growth of nanostructures. Structural and
27 morphological analysis revealed the growth of highly crystalline nanorods with good aspect
28 ratio. The tip deflection in atomic force microscopy revealed a mean output voltage to be 9-
29 9.5 mV. The higher flexibility of textile substrate are expected to increase the voltage
30 manifold [97]. Textile based pressure sensor has also been fabricated using ZnO nanorods.
31 For this purpose, three layers were combined to make a sensor. ZnO nanorods grown on
32 conductive reduced graphene oxide/polyester fabric formed the top and bottom layer, while
33 a PVDF membrane was sandwiched between them. This sensor had a very low detection
34 limit, high sensitivity of 0.62 V/kPa. Further, it produced an open-circuit voltage around
35 11.47 V with superior mechanical stability. This sensor could effectively sense different
36 human motions [98]. There are several studies that have employed ZnO in textile substrates
37 and explored its piezoelectric properties [99,100].
38
39
40
41
42
43
44
45
46
47
48

49 **4.1.3 Film based materials**

50 Piezoelectric films have been prepared by processes like solvent casting, spin coating,
51 supersonic spraying, etc. These methods are facile and suitable for upscaled production.
52 Poling of piezoelectric films helps to improve their piezoelectricity. The combination of
53
54
55
56
57
58
59
60

ZnO and PVDF has been explored extensively in the form of films, prepared through different film preparation techniques. ZnO microrods were synthesized chemically using zinc nitrate and hexamethylenetetramine as precursors. The synthesized microrods were mixed with a solution of PVDF in dimethylformamide (DMF) at different levels of loading. PVDF/ZnO composite films were prepared by supersonic spraying technique. The morphological characterization of films revealed the successful integration of ZnO microrods into PVDF films, while the structural characterizations of the composite films revealed the stabilization and enhancement of electroactive β phase of PVDF. The stretch experienced by the polymer chains during supersonic spraying resulted in the increment of β phase content of PVDF polymer. The d_{33} values obtained for the pristine polymer and composite film showed an increase from 23.3 to 36.3 pm/V, respectively. The output voltage analysis of the fabricated piezoelectric nanogenerator (**Fig. 6**) indicated an increase in the output voltage with increase in ZnO microrod content. However, at higher loading of ZnO, β phase of PVDF decreased that adversely affected the output performance of the composite film. Highest output voltage of 15.2 V and maximum power density of 12.5 $\mu\text{W}/\text{cm}^2$ was obtained for the optimized composition of ZnO/PVDF [101]. In yet another study, ZnO nanoparticles were incorporated in PVDF polymer through spin coating technique. The rough surface of composite film compared to the smooth surface of pristine PVDF film, suggested the successful integration of ZnO nanoparticles into PVDF matrix. Further, elemental analysis carried out through EDS, reaffirmed the presence of the expected elements in the nanocomposite film. The structural analysis through XRD and FTIR indicated the β nucleating effect of the ZnO nanoparticles. The negative charge on the surface of the nanoparticles interacts with the positive charge of the polymer chains to cause the effective nucleation of the β phase. This was further reflected in the enhanced output voltage of 4.2 V for the nanocomposite film compared to 1.2 V for pristine polymer sample [102]. ZnO nanowires were grown hydrothermally on chopped carbon fibre strands. These hierarchical structures were incorporated into spin coated PVDF films. The incorporation of such hierarchical structures in the nanocomposite film helped to enhance its electrical and mechanical performance. The addition of the hierarchical filler to the polymer matrix helped to enhance its electroactive phase. The interfacial polarization between the semiconductor nanowires and the polymer chains deflects the electronegative F atoms to

1
2
3 one side of the polymer chain, stabilizing its β phase conformation. However, too high
4 loading of filler adversely affects the β phase content of the polymer. Dual interface is
5 formed in this nanocomposite film. The interface between ZnO nanowires and polymer
6 matrix influences the formation of β phase of PVDF. Further, the interface between ZnO
7 nanowires and carbon fibre helps in the migration of the polarized charges. The content of
8 filler has a significant effect on the electrical performances. A higher filler content had
9 adversely affected the electrical performance of the nanocomposite films. An optimized
10 amount of filler content helped to achieve a trade-off between the piezoelectric and
11 conductive property, that helped to achieve an output voltage as high as 14.91 V, output
12 current of 1.25 μ A and output power of 7.9 μ W [103]. To improve the piezoelectric property,
13 ZnO nanoparticles were doped with several metal ions and studied for its electrical
14 performance. A 5% Li-doped ZnO has shown striking improvement in its energy harvesting
15 property compared to the same of pristine ZnO. This optimized level of metal doping helped
16 to create defects in the wurtzite structure of ZnO, increasing its asymmetry and thus
17 improving its piezoelectricity. However, a higher level of doping causes screening of
18 piezoelectric charges that adversely affects the piezoelectricity of the doped material. 5%
19 Li-doped ZnO incorporated PVDF-TrFE spin coated porous film generated an output
20 voltage of 3.43 V, compared to 0.38 V for pristine ZnO incorporated PVDF-TrFE spin
21 coated porous film [104]. The size of filler loaded in the composite films also influence the
22 piezoelectric performance of the material. This was explored for PVDF/ZnO nanoparticle
23 incorporated piezoelectric composite. Although the composite performed better compared
24 to the pristine polymer based film, its performance was significantly affected by the size of
25 the filler loaded. The smaller the filler size, the better was the piezoelectric performance of
26 the composite [105].
27
28
29
30
31
32
33
34
35
36
37
38
39
40
41
42
43
44
45
46
47
48
49
50
51
52
53
54
55
56
57
58
59
60

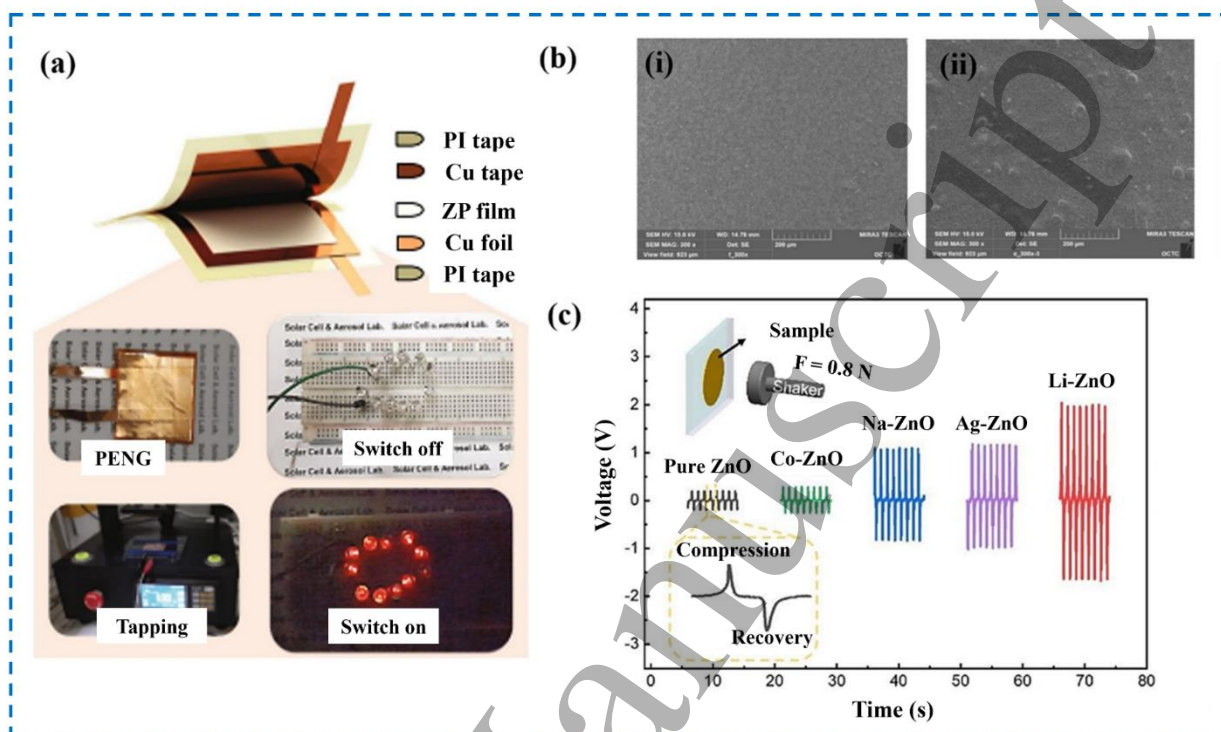


Fig. 6. (a) Fabrication and application of PVDF/ZnO piezoelectric nanogenerator [106] (b)(i) smooth surface of PVDF (ii) rough surface of PVDF/ZnO films [107] (c) voltage output of metal doped ZnO nanoparticles [108] All essential copyrights and permissions taken.

The aspect ratio of fillers, incorporated in a polymer-reinforcement composite, plays a crucial role in governing its electrical properties. To illustrate this, ZnO nanorods with varying aspect ratios were synthesized hydrothermally. Varying the reaction time resulted in synthesis of nanorods with different aspect ratios. The highest reaction time yielded nanorods with the highest aspect ratio and good crystallinity. The study of zeta potential reveals the presence of negative charge on the surface of ZnO nanorods. The higher the aspect ratio, more is the negative charges developed. These negative charges, on the surface of ZnO, interact with the positive CH_2 dipoles of PVDF polymer chains to enhance and stabilize the β phase of PVDF polymer. Thus, incorporation of ZnO nanorods of higher aspect ratio into PVDF polymer helps in enhancing its electroactive phase content. Further, higher aspect ratio of fillers helps in homogeneous dispersion of the filler in the polymer

1
2
3 matrix [109]. ZnO along with other metal oxide nanoparticles have also been incorporated
4 into PVDF to form advanced polymer composites, suitable for electronic device
5 applications [110].
6
7

8 9 **4.2 PVDF/ZnO composite based triboelectric energy harvesting**

10 11 **4.2.1 Electrospun membranes**

12
13
14 TENG is very popular in the field of wasted mechanical energy transduction due to their
15 high electrical power output. Surface decoration with fillers and surface roughening were
16 found to be very effective techniques in improvement of energy harvesting performance of
17 electrospun hybrid nanogenerators [111]. Kim and Fan highlighted the influence of surface
18 roughness on electrical power outputs of nanocomposite fibrous membranes. They have
19 prepared nanocomposite structures using different combinations of ZnO NRs and PVDF
20 matrix. Electrospinning of ZnO and PVDF composite solution was performed to form
21 nanocomposite fibres. Additionally, ZnO NRs were hydrothermally grown and
22 electrospayed onto PVDF electrospun fibres to obtain two different structures. The authors
23 highlighted that with increasing the surface roughness, the power output increases due to
24 triboelectrification (**Fig. 7**) [78].
25
26
27
28
29
30
31
32
33
34
35
36
37
38
39
40
41
42
43
44
45
46
47
48
49
50
51
52
53
54
55
56
57
58
59
60

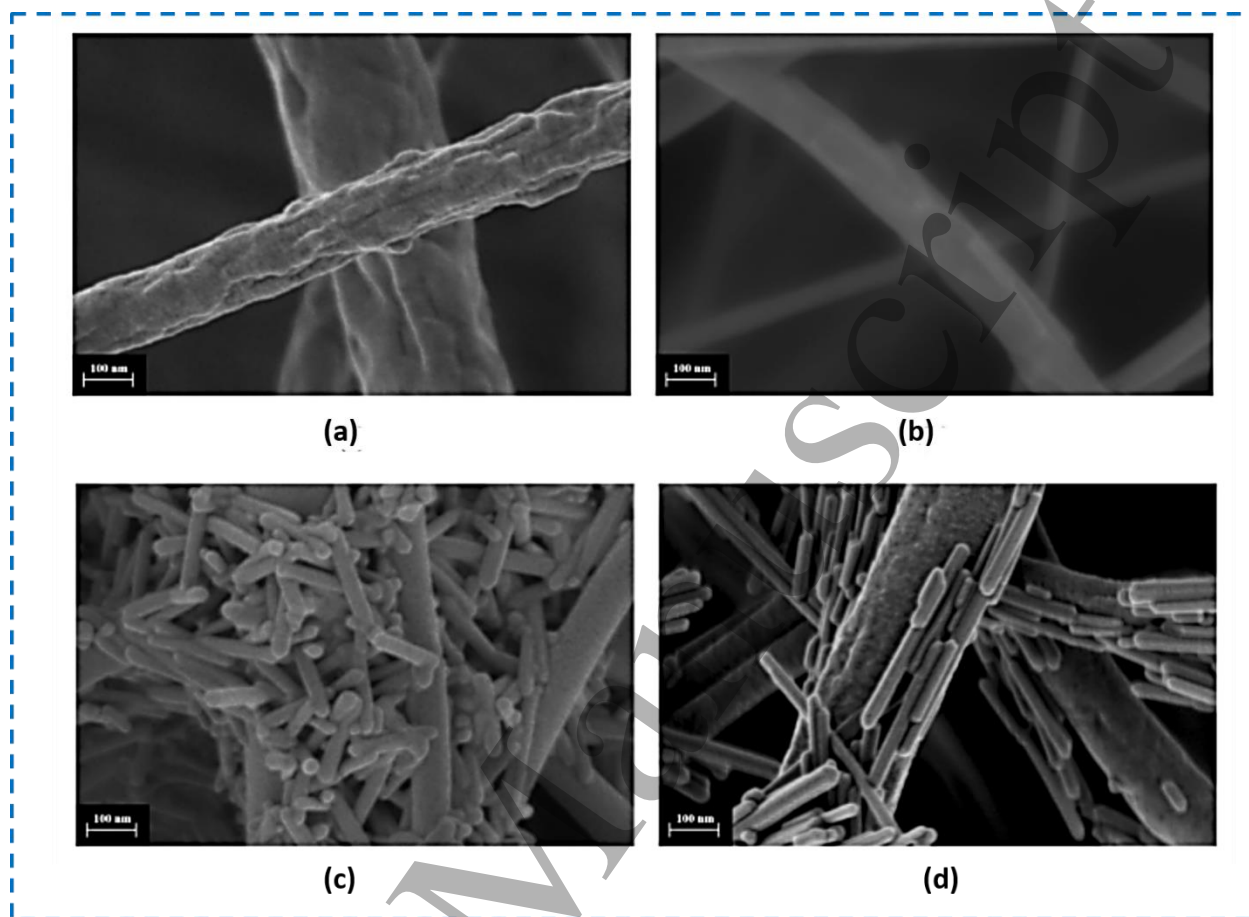


Fig. 7. FESEM images of (a) pristine PVDF nanofibres, (b) (ZnO+PVDF), (c) (ZnO@PVDF), (d) (ZnO/PVDF) [78]

Pu et al. selected two piezoelectric polymers, PVDF and nylon 11, to form different triboelectric layers. Electrospinning technique improves the electroactive phases (β -phase for PVDF and δ' -phase for nylon 11) of the piezoelectric polymer. The addition of ZnO nanowires (NWs) in to PVDF and nylon 11 also improves their respective contents of electroactive phases. Incorporation of ZnO NWs improves the thermal stability, tensile strength and Young's modulus of the composite nanofibres along with reducing the breaking elongation of the same. Triboelectric outputs were found to improve for testing with ZnO loaded PVDF and ZnO loaded nylon 11 as compared to the testing performed using electrospun pristine PVDF and nylon 11 membranes. Approximately four reasons can be found as follows: (i) incorporation of ZnO NWs enhances the electroactive phases of the piezoelectric polymers, (ii) ZnO itself has piezoelectric property which is efficient in conversion of mechanical energy to its electrical counterpart, (iii) improvement in tensile

1
2
3 strength and Young's modulus of the composite membranes can effectively transfer the
4 applied load between the matrix to ZnO NWs, (iv) such alternation in mechanical properties
5 may improve the friction between the triboelectric layers. The authors demonstrated that the
6 developed TENG can lighten over 100 LEDs and charge capacitors of various capacitance
7 values [112]. Li et al. incorporated carbon coated ZnO (ZnO@C) nanoparticles within
8 PVDF electrospun membranes. Increase in the concentration of ZnO@C nanoparticles
9 results in enhancement in β -phase of PVDF as already discussed previously. Due to
10 improvement in polar phase content, the surface potential of the electrospun membrane was
11 also found to alter. As the concentration of nanoparticles increases from 0% to 5 %, the
12 surface potential changes from -130 mV to -740 mV as obtained from Kelvin Probe Force
13 Microscopy (KPFM). Due to improvement in the surface potential in the negative side,
14 triboelectric output voltage also enhances as more potential difference can be created due
15 to higher possibility of charge transfer [82].
16
17
18
19
20
21
22
23
24
25

26 **4.2.2 Film based materials**

27
28 Film-based ZnO-PVDF materials offer advantages over electrospun fibres due to their
29 simplicity, uniformity, durability, and easy integration, making them a cost-effective and
30 customizable choice for various applications, including energy harvesting and sensor
31 technology [113]. This composite excels at converting mechanical energy, such as vibrations
32 and pressure, into electrical energy by combining the intrinsic piezoelectric capabilities of
33 PVDF with the enhanced piezoelectric effect brought about by ZnO nanoparticles [114]. It
34 can be used in a variety of applications, such as wearable electronics and flexible
35 electronics, where it can adapt to diverse surfaces and shapes owing to its strength,
36 flexibility, and wide compatibility with materials [115,116]. Singh and Khare have achieved
37 a noteworthy advancement in the field of triboelectric energy harvesting through their
38 research. By adding ZnO nanorods to the PVDF polymer and combining it with
39 polytetrafluoroethylene (PTFE), they were able to achieve improved triboelectrification
40 (**Fig. 8**). When compared to TENGs manufactured from PVDF/PTFE alone, the resultant
41 ZnO-PVDF/PTFE-based TENG demonstrated impressive performance gains, including a
42 21% rise in output voltage and a significant 60% jump in short-circuit current. Additionally,
43 the remarkable instantaneous output power density of roughly 10.6 mW/cm² was attained
44
45
46
47
48
49
50
51
52
53
54
55
56
57
58
59
60

1
2
3 by this inventive composite. There are several reasons for the increased triboelectrification
4 in this system, one of which is because PVDF has a higher β -phase concentration, which
5 improves polarizability. Furthermore, the incorporation of ZnO nanorods resulted in
6 enhanced hydrophobicity, reduced PVDF work function, and better surface roughness, all
7 of which enhanced TENG performance. Interestingly, the ZnO-PVDF/PTFE-based TENG
8 showed a significant 65.6% increase in output power over the PVDF/PTFE-based TENG,
9 and this improvement was only ascribed to the changes in PVDF's characteristics brought
10 about by the addition of ZnO [113]. TENGs can have their power density greatly increased
11 by using an interfacial piezoelectric ZnO nanosheets layer, as demonstrated in a study by
12 Narasimulu et al. These TENGs were based on phase inversion membranes made of
13 polyamide-6 (PA6) and PVDF. The ZnO nanosheets electrochemically deposited TENG
14 device demonstrated a remarkable output voltage of around 625 V and a current density of
15 about 40 mA/m², which translated into a charge density of roughly 100.6 C/m² when
16 subjected to an applied force of 80 N. In comparison to the pure TENG device, which
17 produced an output voltage of about 310 V, a current density of about 10 mA/m², and a
18 charge density of about 77.45 C/m², this represented an improvement. Under compressive
19 stress, the ZnO nanosheets produced a piezoelectric potential that injected charge onto the
20 ZnSnO₃-PVDF membrane's surface, leading to improved charge density and a substantial
21 increase in power density from 0.11 to approximately 1.8 W/m². This research underscores
22 the potential for using interfacial piezoelectric ZnO nanosheets to enhance energy
23 harvesting and power generation in TENG devices [117]. The efficiency of triboelectric
24 energy harvesting could be revolutionized by modern materials and nanotechnology.
25 Optimizing the combination of PVDF and ZnO for maximum energy conversion, ensuring
26 long-term durability, and establishing standardized testing methods are essential steps to
27 realize the full potential of this energy harvesting technology.
28
29
30
31
32
33
34
35
36
37
38
39
40
41
42
43
44
45
46
47
48
49
50
51
52
53
54
55
56
57
58
59
60

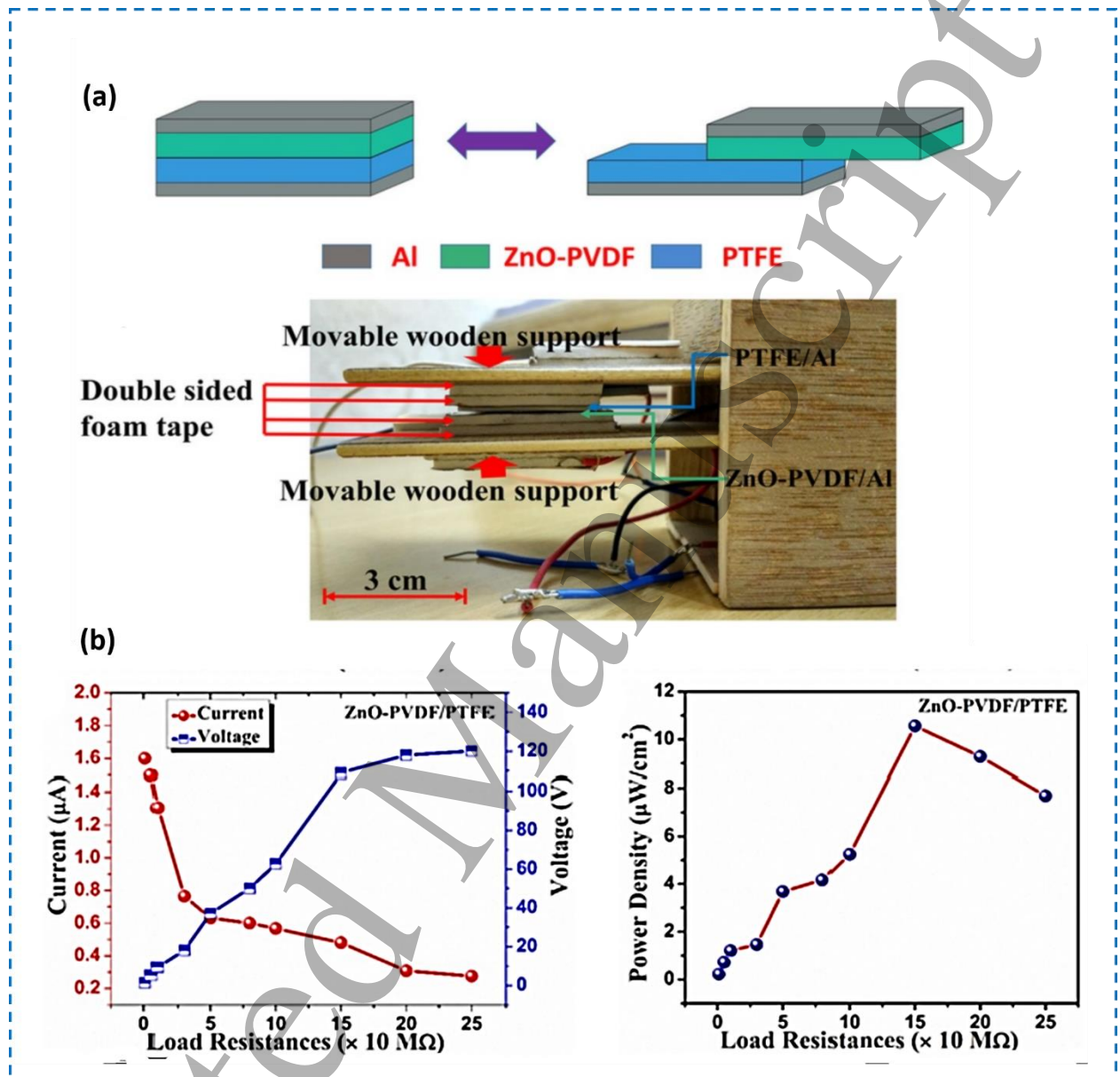


Figure 8: (a) Schematic of the fabricated ZnO-PVDF/PTFE-based TENG showing in-plane separation. (b) The respective instantaneous output power density with the different load resistance of PVDF/PTFE and ZnO-PVDF/PTFE-based TENG [113]. All essential copyrights and permissions taken.

Hybrid nanogenerators based on PVDF and ZnO constitute a noteworthy development in energy harvesting technology. Through the integration of ZnO's semiconducting characteristic and PVDF's piezoelectric quality, these nanogenerators effectively transform mechanical energy into electrical power. They provide sustainable and independent energy

1
2
3 solutions for a variety of applications, including wearable electronics and self-powered
4 sensors, due to their adaptable and versatile design [118]. By producing a ZnO-PVDF film
5 and combining it with PTFE to create a piezo-tribo-based hybrid nanogenerator, Singh and
6 Khare have made a noteworthy advancement. Their investigation showed that adding ZnO
7 to the PVDF matrix improves the material's triboelectric qualities in addition to its
8 piezoelectric one. As a result of this breakthrough, a ZnO-PVDF-based piezo-tribo hybrid
9 generator was created that can produce an impressive 2.5 times more power than a bare
10 PVDF-based hybrid nanogenerator, with an instantaneous maximum output power of
11 roughly $24.5 \mu\text{W}/\text{cm}^2$. The noteworthy aspect of this enhancement is that it was achieved
12 without the need for surface treatment or electrical poling, solely by introducing ZnO
13 nanorods into the PVDF matrix [119]. This pioneering approach represents a promising
14 direction for simultaneously harnessing the piezoelectric and triboelectric energies from a
15 single device, offering new opportunities for efficient energy harvesting.
16
17
18
19
20
21
22
23
24
25

26 **5. Challenges and future look**

27
28 Advancements in nanotechnology and nano-manufacturing techniques are set to
29 revolutionize the production of nanogenerators, enabling large-scale and cost-effective
30 manufacturing. The integration of nanogenerators into everyday objects, such as clothing,
31 sensors, and infrastructure, offers a vast array of potential applications, from self-powered
32 wearables to smart cities. Moreover, the ongoing standardization efforts and the
33 establishment of industry guidelines will pave the way for widespread adoption and
34 commercialization. There are particular difficulties with both PENGs and TENGs.
35 Regarding PVDF-ZnO composites, the main challenges are related to material and design,
36 including developing mechanical structures to maximize energy conversion efficiency and
37 optimizing materials to boost their piezoelectric coefficients. Furthermore, it is critical to
38 guarantee scalability and endurance for these composites to be appropriate for a variety of
39 uses, such as wearable technologies and large-scale energy harvesting systems.
40 Interestingly, PVDF-ZnO based TENGs have a unique set of characteristics. The coupling
41 of two complementary materials with differing triboelectric charge densities results in
42 creation of a large potential difference leading to generation of high electrical output.
43
44
45
46
47
48
49
50
51
52
53
54
55
56
57
58
59
60

1
2
3 Ensuring TENG durability and long-term performance is a persistent concern, particularly
4 in high-friction situations.
5

6
7 PVDF-ZnO composite advancements are about to take a radical turn because of the
8 development of artificial intelligence (AI) and machine learning (ML). Large-scale material
9 property information can be analyzed by AI algorithms to find the best candidates for PENG
10 and TENG applications, maximizing their effectiveness. To ensure that these
11 nanogenerators run as efficiently as possible, ML models can be used to further optimize
12 their configuration and design. Furthermore, PVDF-ZnO composite-based nanogenerators
13 will have a longer lifespan and higher overall efficiency thanks to AI-driven predictive
14 maintenance algorithms. The creation of novel materials, creative designs, and a wide range
15 of applications is expected to accelerate with the integration of AI and ML, increasing the
16 efficiency and adaptability of PVDF-ZnO composites to a variety of scenarios and sectors.
17
18

19
20
21 When a piezoelectric material is being used as a triboelectric surface, there is obviously a
22 possibility of getting piezoelectric voltage output along with triboelectric output. Similarly,
23 during characterization of piezoelectricity out of a piezoelectric material, there is every
24 possibility that triboelectric voltage also arises due to friction between two different
25 materials. Sutka et al. stated that often triboelectric output is misinterpreted as piezoelectric
26 output ultimately reporting irreproducible piezoelectric coefficients. The authors reported
27 that in a piezoelectric generator contact electrification may arise from static discharge from
28 rubber glove or human finger, commonly used to test piezoelectric energy harvesting
29 efficiency. Additionally, shear force within a composite and friction between interfaces also
30 result in triboelectrification within a piezoelectric generator. Device fabrication technique,
31 testing apparatus, low resistance electrical measuring instruments and external circuitry can
32 introduce deceptive results within a true piezoelectric output [120–122]. Very few
33 researchers investigated the paths of differentiating the true piezoelectric output from the
34 unwanted triboelectric one. Musa et al. confirmed that triboelectric signal can be bipolar in
35 contact and unipolar in separation in a course of contact-separation cycle [57]. This
36 phenomenon is obviously a unique signature of triboelectrification, distinguishing it from
37 piezoelectric signal. Sutka et al. reported that incorporation of conductive tape in-between
38 the electrode and polymeric substrate can neutralise the unwanted charges arising from
39
40
41
42
43
44
45
46
47
48
49
50
51
52
53
54
55
56
57
58
59
60

1
2
3 contact-electrification. A piezoelectric polymer with sputtered electrodes can be
4 encapsulated with the help of thin dielectric layer. Thereafter, this device can be coated with
5 a flexible grounded conducting material to dissipate the charges generated due to friction.
6 Additionally, if a piezoelectric material is compressed and released periodically without
7 breaking the contact between piezoelectric substrate and the force imparting object,
8 negligible contact electrification can be expected from the contact-separation between these
9 two parts [120]. Suo et al. mentioned that electrical pulse for piezoelectricity and the same
10 for triboelectricity can be distinguished by their natures. Peak for triboelectricity is sharp
11 and narrow whereas the same for piezoelectricity is relatively broad due to strain induced
12 charge generation. The authors also argued that total electrical output is addition of the
13 outputs of piezoelectricity and triboelectricity [122]. During piezoelectric energy harvesting
14 obviously we need another object to exert force onto the piezoelectric material. Contact-
15 separation cycles between this object and piezoelectric device lead to triboelectric charge
16 generation. Chen et al. stated that triboelectric signal generates in three stages, namely:
17 contacting, contacted and separating. On the other hand, piezoelectric signal generates in
18 contacted stage which further can be subdivided into compressing, compressed and
19 releasing stages. More specifically, triboelectric signals mainly appear before and after the
20 contact between the object and piezoelectric device whereas the piezoelectric signal arises
21 during contact between the object and piezoelectric device. By analysing the force signal
22 and electrical signal, both the responses from piezoelectricity and triboelectricity can be
23 identified in a systematic manner. Moreover, the authors also developed a technique to
24 mathematically quantify the piezoelectric output from a hybrid signal [123]. So, there is high
25 chance that the perceived piezoelectric output has a hidden triboelectric component within
26 it. Research should be done to separate these two outputs and quantification of actual
27 piezoelectric and triboelectric outputs is of vital importance.
28
29
30
31
32
33
34
35
36
37
38
39
40
41
42
43
44
45
46
47
48

49 **Conclusion**

50
51 Due to the present concern of energy crisis, the need for renewable energy sources is
52 amplifying day by day. Sources of mechanical energy are numerous, and this kind of energy
53 is being wasted in various forms. For these reasons, there is a growing concern of conversion
54
55
56
57
58
59
60

of these mechanical energies into electrical one for powering small electronics. Piezoelectricity and triboelectricity, two scientific phenomena, have come out to be very efficient in this respect. Proper material selection and fabrication of an ideal structure out of them are the bases of piezoelectric and triboelectric device manufacturing. Piezoelectric materials can be broadly classified into single crystals, ceramics, polymers and composites. Each class has its own benefits and disadvantages. In order to partially overcome the limitations of each constituent along with obtaining the respective benefits of the same, piezoelectric ceramics are often combined with polymers to obtain piezoelectric composites, having enhanced property compared to its constituent materials. PVDF is a well-known piezoelectric polymer for its high piezoelectric property among the piezoelectric polymers. PVDF offers various phases depending on its chemical conformations. β -phase, an electroactive phase, of PVDF is known to be primarily responsible for piezoelectric performance of PVDF. Incorporation of small amount of filler into PVDF matrix has proved to be effective for generation of β -phase of PVDF. In this context, ZnO was found to enhance the piezoelectric performance of PVDF. ZnO is known for its functionalities like piezoelectricity, pyroelectricity, anti-bacterial activity, ultraviolet protection. Different nanostructures of ZnO can be easily prepared using various routes. Apart from improving the electroactive phase of PVDF, addition of ZnO into PVDF matrix can enhance the mechanical energy harvesting performance due to several other effects. The piezoelectric property of ZnO itself contributes to the overall electrical performance of PVDF-ZnO composite. Incorporation of ZnO within PVDF results in an increase in surface roughness of the composite structure thereby improving the triboelectric performance of the resultant material. Although there is good number of research on mechanical energy harvesting of electrospun PVDF-ZnO composites but number of research related to energy harvesting performance of this particular composite in other structural forms is still less. PVDF-ZnO hybrid material has proven to be very efficient not only in wasted mechanical energy harvesting but also it performs significantly in sensing and disease detection areas.

Acknowledgements

Authors are grateful to the Department of Science and Technology and The Government of India for funding the work on piezoelectric device development and as a part of that the

1
2
3 authors have prepared this review article (Sanction Letter: DST/TDT/DDP-05/2018 (G))
4 under Device Development Program). The authors would also like to acknowledge the
5 support of the UK Engineering and Physical Sciences Research Council (EPSRC) through
6 grant Ref. EP/V003380/1: ‘Next Generation Energy Autonomous Textile Fabrics based on
7 Triboelectric Nanogenerators’.
8
9
10
11
12
13
14

15 Reference

- 16
17 [1] Lampert A. Over-exploitation of natural resources is followed by inevitable declines in
18 economic growth and discount rate. *Nat Commun* 2019;10:1–10.
19 <https://doi.org/10.1038/s41467-019-09246-2>.
20
21 [2] Cao S, Li J. A survey on ambient energy sources and harvesting methods for structural
22 health monitoring applications. *Advances in Mechanical Engineering* 2017;9:1–14.
23 <https://doi.org/10.1177/1687814017696210>.
24
25 [3] Prauzek M, Konecny J, Borova M, Janosova K, Hlavica J, Musilek P. Energy harvesting
26 sources, storage devices and system topologies for environmental wireless sensor
27 networks: A review. *Sensors (Switzerland)* 2018;18. <https://doi.org/10.3390/s18082446>.
28
29 [4] Khan U, Kim SW. Triboelectric Nanogenerators for Blue Energy Harvesting. *ACS Nano*
30 2016;10:6429–32. <https://doi.org/10.1021/acsnano.6b04213>.
31
32 [5] Zou Y, Raveendran V, Chen J. Wearable triboelectric nanogenerators for biomechanical
33 energy harvesting. *Nano Energy* 2020;77:105303.
34 <https://doi.org/10.1016/j.nanoen.2020.105303>.
35
36 [6] Pang Y, Cao Y, Derakhshani M, Fang Y, Wang ZL, Cao C. Hybrid Energy-Harvesting Systems
37 Based on Triboelectric Nanogenerators. *Matter* 2021;4:116–43.
38 <https://doi.org/10.1016/j.matt.2020.10.018>.
39
40 [7] Covaci C, Gontean A. Piezoelectric energy harvesting solutions: A review. *Sensors*
41 (Switzerland) 2020;20:1–37. <https://doi.org/10.3390/s20123512>.
42
43 [8] Toprak A, Tigli O. Piezoelectric energy harvesting : State-of-the-art and challenges. *Applied*
44 *Physics Reviews* 1 2014;031104:1–14. <https://doi.org/10.1063/1.4896166>.
45
46 [9] Sezer N, Koç M. A comprehensive review on the state-of-the-art of piezoelectric energy
47 harvesting. *Nano Energy* 2021;80:105567.
48 <https://doi.org/10.1016/j.nanoen.2020.105567>.
49
50 [10] Zou H, Guo L, Xue H, Zhang Y, Shen X, Liu X, et al. Quantifying and understanding the
51 triboelectric series of inorganic non-metallic materials. *Nat Commun* 2020;11:1–7.
52 <https://doi.org/10.1038/s41467-020-15926-1>.
53
54
55
56
57
58
59
60

- 1
2
3 [11] Kim DW, Lee JH, Kim JK, Jeong U. Material aspects of triboelectric energy generation and
4 sensors. *NPG Asia Mater* 2020;12. <https://doi.org/10.1038/s41427-019-0176-0>.
5
6 [12] Wang N, Liu Y, Ye E, Li Z, Wang D. Control methods and applications of interface contact
7 electrification of triboelectric nanogenerators: a review. *Mater Res Lett* 2022;10:97–123.
8 <https://doi.org/10.1080/21663831.2022.2026513>.
9
10 [13] Banerjee S, Bairagi S, Wazed Ali S. A critical review on lead-free hybrid materials for next
11 generation piezoelectric energy harvesting and conversion. *Ceram Int* 2021;47:16402–21.
12 <https://doi.org/10.1016/j.ceramint.2021.03.054>.
13
14 [14] Bairagi S, Ali SW. Flexible lead-free PVDF / SM-KNN electrospun nanocomposite based
15 piezoelectric materials : Signi fi cant enhancement of energy harvesting ef fi ciency of the
16 nanogenerator. *Energy* 2020;198:117385. <https://doi.org/10.1016/j.energy.2020.117385>.
17
18 [15] Bairagi S, Ali SW. Effects of surface modification on electrical properties of KNN nanorod-
19 incorporated PVDF composites. *J Mater Sci* 2019;54:11462–84.
20 <https://doi.org/10.1007/s10853-019-03719-x>.
21
22 [16] Bairagi S, Ali SW. Poly (vinylidene fluoride) (PVDF)/Potassium Sodium Niobate (KNN)
23 nanorods based flexible nanocomposite film; Influence of KNN concentration in the
24 performance of nanogenerator. *Org Electron* 2020;78:105547.
25 <https://doi.org/10.1016/j.orgel.2019.105547>.
26
27 [17] Park K Il, Jeong CK, Kim NK, Lee KJ. Stretchable piezoelectric nanocomposite generator.
28 *Nano Converg* 2016;3:1–12. <https://doi.org/10.1186/s40580-016-0072-z>.
29
30 [18] Zhao Y, Liao Q, Zhang G, Zhang Z, Liang Q, Liao X, et al. High output piezoelectric
31 nanocomposite generators composed of oriented BaTiO₃ NPs at PVDF. *Nano Energy*
32 2015;11:719–27. <https://doi.org/10.1016/j.nanoen.2014.11.061>.
33
34 [19] Jiyong H, Yuanyuan G, Hele Z, Yinda Z, Xudong Y. Effect of electrospinning parameters on
35 piezoelectric properties of electrospun PVDF nanofibrous mats under cyclic compression.
36 *Journal of the Textile Institute* 2018;109:843–50.
37 <https://doi.org/10.1080/00405000.2017.1377882>.
38
39 [20] Cozza ES, Monticelli O, Marsano E, Cebe P. On the electrospinning of PVDF: Influence of
40 the experimental conditions on the nanofiber properties. *Polym Int* 2013;62:41–8.
41 <https://doi.org/10.1002/pi.4314>.
42
43 [21] Zhang X, Xia W, Liu J, Zhao M, Li M, Xing J. PVDF-based and its Copolymer-Based
44 Piezoelectric Composites: Preparation Methods and Applications. *J Electron Mater*
45 2022;51:5528–49. <https://doi.org/10.1007/s11664-022-09825-y>.
46
47 [22] Jiang L, Xie H, Hou Y, Wang S, Xia Y, Li Y, et al. Enhanced piezoelectricity of a PVDF-based
48 nanocomposite utilizing high-yield dispersions of exfoliated few-layer MoS₂. *Ceram Int*
49 2019;45:11347–52. <https://doi.org/10.1016/j.ceramint.2019.02.213>.
50
51
52
53
54
55
56
57
58
59
60

- 1
2
3 [23] Jiang J, Tu S, Fu R, Li J, Hu F, Yan B, et al. Flexible Piezoelectric Pressure Tactile Sensor
4 Based on Electrospun BaTiO₃/Poly(vinylidene fluoride) Nanocomposite Membrane. ACS
5 Appl Mater Interfaces 2020;12:33989–98. <https://doi.org/10.1021/acsami.0c08560>.
6
7 [24] Bairagi S, Ali SW. Flexible lead-free PVDF/SM-KNN electrospun nanocomposite based
8 piezoelectric materials: Significant enhancement of energy harvesting efficiency of the
9 nanogenerator. Energy 2020;198:117385. <https://doi.org/10.1016/j.energy.2020.117385>.
10
11 [25] Mirzazadeh Z, Sherafat Z, Bagherzadeh E. Physical and mechanical properties of
12 PVDF/KNN composite produced via hot compression molding. Ceram Int 2021;47:6211–9.
13 <https://doi.org/10.1016/j.ceramint.2020.10.199>.
14
15 [26] Shoorangiz M, Sherafat Z, Bagherzadeh E. CNT loaded PVDF-KNN nanocomposite films
16 with enhanced piezoelectric properties. Ceram Int 2022;48:15180–8.
17 <https://doi.org/10.1016/j.ceramint.2022.02.047>.
18
19 [27] Cochran S. Piezoelectricity and basic configurations for piezoelectric ultrasonic
20 transducers. Ultrasonic Transducers: Materials and Design for Sensors, Actuators and
21 Medical Applications 2012:3–35. <https://doi.org/10.1533/9780857096302.1.3>.
22
23 [28] Wu J. Perovskite lead-free piezoelectric ceramics. J Appl Phys 2020;127:190901.
24 <https://doi.org/10.1063/5.0006261>.
25
26 [29] Zheng H, Wang Y, Liu J, wang J, Yan K, Zhu K. Recent advancements in the use of novel
27 piezoelectric materials for piezocatalytic and piezo-photocatalytic applications. Appl Catal
28 B 2024;341:123335. <https://doi.org/10.1016/j.apcatb.2023.123335>.
29
30 [30] Yang J, Chen J, Yang Y, Zhang H, Yang W, Bai P, et al. Broadband vibrational energy
31 harvesting based on a triboelectric nanogenerator. Adv Energy Mater 2014;4:1–9.
32 <https://doi.org/10.1002/aenm.201301322>.
33
34 [31] Mukhopadhyay SC. Wearable sensors for human activity monitoring: A review. IEEE Sens J
35 2015;15:1321–30. <https://doi.org/10.1109/JSEN.2014.2370945>.
36
37 [32] Yang Y, Guo W, Pradel KC, Zhu G, Zhou Y, Zhang Y, et al. Pyroelectric nanogenerators for
38 harvesting thermoelectric energy. Nano Lett 2012;12:2833–8.
39 <https://doi.org/10.1021/nl3003039>.
40
41 [33] Wang Y, Yang Y, Wang ZL. Triboelectric nanogenerators as flexible power sources. Npj
42 Flexible Electronics 2017;1:1–9. <https://doi.org/10.1038/s41528-017-0007-8>.
43
44 [34] Adapa A, Nah FFH, Hall RH, Siau K, Smith SN. Factors Influencing the Adoption of Smart
45 Wearable Devices. Int J Hum Comput Interact 2018;34:399–409.
46 <https://doi.org/10.1080/10447318.2017.1357902>.
47
48 [35] Wang ZL, Song J. Piezoelectric nanogenerators based on zinc oxide nanowire arrays.
49 Science (1979) 2006;312:242–6. <https://doi.org/10.1126/science.1124005>.
50
51
52
53
54
55
56
57
58
59
60

- 1
2
3 [36] Suyitno, Hadi S, Sahdan MZ, Nayan N, Saim H, Nulhakim L, et al. Simple Fabrication and
4 Characterization of Piezoelectric Nanogenerators from Cobalt-Doped Zinc Oxide
5 Nanofibers. *Am J Appl Sci* 2017;14:662–9. <https://doi.org/10.3844/ajassp.2017.662.669>.
6
7 [37] Shi K, Zou H, Sun B, Jiang P, He J, Huang X. Dielectric Modulated Cellulose Paper/PDMS-
8 Based Triboelectric Nanogenerators for Wireless Transmission and Electropolymerization
9 Applications. *Adv Funct Mater* 2020;30:1–9. <https://doi.org/10.1002/adfm.201904536>.
10
11 [38] Kim I, Jeon H, Kim D, You J, Kim D. All-in-one cellulose based triboelectric nanogenerator
12 for electronic paper using simple filtration process. *Nano Energy* 2018;53:975–81.
13 <https://doi.org/10.1016/j.nanoen.2018.09.060>.
14
15 [39] Han J, Liu Y, Feng Y, Jiang T, Wang ZL. Achieving a Large Driving Force on Triboelectric
16 Nanogenerator by Wave-Driven Linkage Mechanism for Harvesting Blue Energy toward
17 Marine Environment Monitoring. *Adv Energy Mater* 2023;13.
18 <https://doi.org/10.1002/aenm.202203219>.
19
20 [40] Shi Q, Wang H, Wu H, Lee C. Self-powered triboelectric nanogenerator buoy ball for
21 applications ranging from environment monitoring to water wave energy farm. *Nano*
22 *Energy* 2017;40:203–13. <https://doi.org/10.1016/j.nanoen.2017.08.018>.
23
24 [41] Zhu G, Pan C, Guo W, Chen CY, Zhou Y, Yu R, et al. Triboelectric-generator-driven pulse
25 electrodeposition for micropatterning. *Nano Lett* 2012;12:4960–5.
26 <https://doi.org/10.1021/nl302560k>.
27
28 [42] Li GZ, Wang GG, Ye DM, Zhang XW, Lin ZQ, Zhou HL, et al. High-Performance Transparent
29 and Flexible Triboelectric Nanogenerators Based on PDMS-PTFE Composite Films. *Adv*
30 *Electron Mater* 2019;5:1–8. <https://doi.org/10.1002/aelm.201800846>.
31
32 [43] Xia K, Zhu Z, Zhang H, Xu Z. A triboelectric nanogenerator as self-powered temperature
33 sensor based on PVDF and PTFE 2018:2–8.
34
35 [44] Yang Y, Zhang H, Lin ZH, Zhou YS, Jing Q, Su Y, et al. Human skin based triboelectric
36 nanogenerators for harvesting biomechanical energy and as self-powered active tactile
37 sensor system. *ACS Nano* 2013;7:9213–22. <https://doi.org/10.1021/nn403838y>.
38
39 [45] Fan FR, Tian ZQ, Lin Wang Z. Flexible triboelectric generator. *Nano Energy* 2012;1:328–34.
40 <https://doi.org/10.1016/j.nanoen.2012.01.004>.
41
42 [46] Zhang R, Olin H. Material choices for triboelectric nanogenerators: A critical review.
43 *EcoMat* 2020;2:1–13. <https://doi.org/10.1002/eom2.12062>.
44
45 [47] Yao C, Yin X, Yu Y, Cai Z, Wang X. Chemically Functionalized Natural Cellulose Materials for
46 Effective Triboelectric Nanogenerator Development. *Adv Funct Mater* 2017;27:1–7.
47 <https://doi.org/10.1002/adfm.201700794>.
48
49 [48] Shao J, Willatzen M, Wang ZL. Theoretical modeling of triboelectric nanogenerators
50 (TENGs). *J Appl Phys* 2020;128. <https://doi.org/10.1063/5.0020961>.
51
52
53
54
55
56
57
58
59
60

- 1
2
3 [49] Niu S, Wang ZL. Theoretical systems of triboelectric nanogenerators. *Nano Energy* 2014;14:161–92. <https://doi.org/10.1016/j.nanoen.2014.11.034>.
- 4
5
6 [50] Liang X, Jiang T, Feng Y, Lu P, An J, Wang ZL. Triboelectric Nanogenerator Network
7 Integrated with Charge Excitation Circuit for Effective Water Wave Energy Harvesting. *Adv*
8 *Energy Mater* 2020;10:1–8. <https://doi.org/10.1002/aenm.202002123>.
- 9
10 [51] Khandelwal G, Maria Joseph Raj NP, Kim SJ. Materials Beyond Conventional Triboelectric
11 Series for Fabrication and Applications of Triboelectric Nanogenerators. *Adv Energy Mater*
12 2021;11:1–32. <https://doi.org/10.1002/aenm.202101170>.
- 13
14 [52] Li J, Long Y, Yang F, Wang X. Respiration-driven triboelectric nanogenerators for
15 biomedical applications. *EcoMat* 2020;2. <https://doi.org/10.1002/eom2.12045>.
- 16
17 [53] Zhang N, Tao C, Fan X, Chen J. Progress in triboelectric nanogenerators as self-powered
18 smart sensors. *J Mater Res* 2017;32:1628–46. <https://doi.org/10.1557/jmr.2017.162>.
- 19
20 [54] Seol ML, Woo JH, Jeon SB, Kim D, Park SJ, Hur J, et al. Vertically stacked thin triboelectric
21 nanogenerator for wind energy harvesting. *Nano Energy* 2015;14:201–8.
22 <https://doi.org/10.1016/j.nanoen.2014.11.016>.
- 23
24 [55] Holterman J, Groen P. *An Introduction to Piezoelectric Materials and Components*. 2018.
- 25
26 [56] Zhang C, Fan W, Wang S, Wang Q, Zhang Y, Dong K. Recent Progress of Wearable
27 Piezoelectric Nanogenerators. *ACS Appl Electron Mater* 2021;3:2449–67.
28 <https://doi.org/10.1021/acsaelm.1c00165>.
- 29
30 [57] Musa UG, Cezan SD, Baytekin B, Baytekin HT. The Charging Events in Contact-Separation
31 Electrification. *Sci Rep* 2018;8:1–8. <https://doi.org/10.1038/s41598-018-20413-1>.
- 32
33 [58] Zhang X, Chen L, Jiang Y, Lim W, Soh S. Rationalizing the Triboelectric Series of Polymers.
34 *Chemistry of Materials* 2019;31:1473–8.
35 <https://doi.org/10.1021/acs.chemmater.8b04526>.
- 36
37 [59] Zou H, Guo L, Xue H, Zhang Y, Shen X, Liu X, et al. Quantifying and understanding the
38 triboelectric series of inorganic non-metallic materials. *Nat Commun* 2020;11:1–7.
39 <https://doi.org/10.1038/s41467-020-15926-1>.
- 40
41 [60] Yao L, Zhang H, Jiang J, Zhang Z, Zheng X. Recent Progress in Sensing Technology Based on
42 Triboelectric Nanogenerators in Dynamic Behaviors. *Sensors* 2022;22.
43 <https://doi.org/10.3390/s22134837>.
- 44
45 [61] Nivedhitha DM, Jeyanthi S. Polyvinylidene fluoride, an advanced futuristic smart polymer
46 material: A comprehensive review. *Polym Adv Technol* 2023;34:474–505.
47 <https://doi.org/10.1002/pat.5914>.
- 48
49 [62] Kim GH, Hong SM, Seo Y. Piezoelectric properties of poly(vinylidene fluoride) and carbon
50 nanotube blends: β -phase development. *Physical Chemistry Chemical Physics*
51 2009;11:10506–12. <https://doi.org/10.1039/b912801h>.
- 52
53
54
55
56
57
58
59
60

- 1
2
3 [63] Wu L, Jin Z, Liu Y, Ning H, Liu X, Alamusi, et al. Recent advances in the preparation of
4 PVDF-based piezoelectric materials. *Nanotechnol Rev* 2022;11:1386–407.
5 <https://doi.org/10.1515/ntrev-2022-0082>.
6
7 [64] Lee JP, Lee JW, Baik JM. The progress of PVDF as a functional material for triboelectric
8 nanogenerators and self-powered sensors. *Micromachines (Basel)* 2018;9:30–3.
9 <https://doi.org/10.3390/mi9100532>.
10
11 [65] Vu DL, Ahn KK. Triboelectric Enhancement of Polyvinylidene Fluoride Membrane Using
12 Magnetic Nanoparticle for Water-Based Energy Harvesting. *Polymers (Basel)* 2022;14.
13 <https://doi.org/10.3390/polym14081547>.
14
15 [66] Lee JP, Lee JW, Baik JM. The progress of PVDF as a functional material for triboelectric
16 nanogenerators and self-powered sensors. *Micromachines (Basel)* 2018;9:30–3.
17 <https://doi.org/10.3390/mi9100532>.
18
19 [67] Ong DTK, Koay JSC, Sim MT, Aw KC, Nakajima T, Chen BH, et al. High performance
20 composition-tailored PVDF triboelectric nanogenerator enabled by low temperature-
21 induced phase transition. *Nano Energy* 2023;113:108555.
22 <https://doi.org/10.1016/j.nanoen.2023.108555>.
23
24 [68] Wang Y, Zhu L, Du C. Progress in piezoelectric nanogenerators based on pvdf composite
25 films. *Micromachines (Basel)* 2021;12. <https://doi.org/10.3390/mi12111278>.
26
27 [69] Long YZ, Yan X, Wang XX, Zhang J, Yu M. ELECTROSPINNING: THE SETUP AND PROCEDURE.
28 *Electrospinning: Nanofabrication and Applications*, Elsevier Inc.; 2019, p. 21–52.
29 <https://doi.org/10.1016/B978-0-323-51270-1.00002-9>.
30
31 [70] Jiyong H, Yinda Z, Hele Z, Yuanyuan G, Xudong Y. Mixed effect of main electrospinning
32 parameters on the β -phase crystallinity of electrospun PVDF nanofibers. *Smart Mater*
33 *Struct* 2017;26. <https://doi.org/10.1088/1361-665X/aa7245>.
34
35 [71] Martins P, Lopes AC, Lanceros-Mendez S. Electroactive phases of poly(vinylidene fluoride):
36 Determination, processing and applications. *Prog Polym Sci* 2014;39:683–706.
37 <https://doi.org/10.1016/j.progpolymsci.2013.07.006>.
38
39 [72] Goel S, Kumar B. A review on piezo-/ferro-electric properties of morphologically diverse
40 ZnO nanostructures. *J Alloys Compd* 2020;816:152491.
41 <https://doi.org/10.1016/j.jallcom.2019.152491>.
42
43 [73] Momeni K, Odegard GM, Yassar RS. Finite size effect on the piezoelectric properties of
44 ZnO nanobelts: A molecular dynamics approach. *Acta Mater* 2012;60:5117–24.
45 <https://doi.org/10.1016/j.actamat.2012.06.041>.
46
47 [74] Xiang HJ, Yang J, Hou JG, Zhu Q. Piezoelectricity in ZnO nanowires: A first-principles study.
48 *Appl Phys Lett* 2006;89. <https://doi.org/10.1063/1.2397013>.
49
50 [75] Udom I, Ram MK, Stefanakos EK, Hepp AF, Goswami DY. One dimensional-ZnO
51 nanostructures: Synthesis, properties and environmental applications. *Mater Sci*
52 *Semicond Process* 2013;16:2070–83. <https://doi.org/10.1016/j.mssp.2013.06.017>.
53
54
55
56
57
58
59
60

- 1
2
3 [76] Noman MT, Amor N, Petru M. Synthesis and applications of ZnO nanostructures (ZONs):
4 a review. *Critical Reviews in Solid State and Materials Sciences* 2022;47:99–141.
5 <https://doi.org/10.1080/10408436.2021.1886041>.
6
7 [77] Costa LMM, Bretas RES, Gregorio R. Effect of Solution Concentration on the
8 Electro Spray/Electrospinning Transition and on the Crystalline Phase of PVDF. *Materials*
9 *Sciences and Applications* 2010;01:247–52. <https://doi.org/10.4236/msa.2010.14036>.
10
11 [78] Kim M, Fan J. Piezoelectric Properties of Three Types of PVDF and ZnO Nanofibrous
12 Composites. *Advanced Fiber Materials* 2021;3:160–71. [https://doi.org/10.1007/s42765-](https://doi.org/10.1007/s42765-021-00068-w)
13 [021-00068-w](https://doi.org/10.1007/s42765-021-00068-w).
14
15 [79] Yang T, Pan H, Tian G, Zhang B, Xiong D, Gao Y, et al. Hierarchically structured PVDF/ZnO
16 core-shell nanofibers for self-powered physiological monitoring electronics. *Nano Energy*
17 2020;72:104706. <https://doi.org/10.1016/j.nanoen.2020.104706>.
18
19 [80] Feng W, Chen Y, Wang W, Yu D. A waterproof and breathable textile pressure sensor with
20 high sensitivity based on PVDF/ZnO hierarchical structure. *Colloids Surf A Physicochem*
21 *Eng Asp* 2022;633:127890. <https://doi.org/10.1016/j.colsurfa.2021.127890>.
22
23 [81] Mahanty B, Ghosh SK, Jana S, Mallick Z, Sarkar S, Mandal D. ZnO nanoparticle confined
24 stress amplified all-fiber piezoelectric nanogenerator for self-powered healthcare
25 monitoring. *Sustain Energy Fuels* 2021;5:4389–400. <https://doi.org/10.1039/d1se00444a>.
26
27 [82] Li X, Ji D, Yu B, Ghosh R, He J, Qin X, et al. Boosting piezoelectric and triboelectric effects
28 of PVDF nanofiber through carbon-coated piezoelectric nanoparticles for highly sensitive
29 wearable sensors. *Chemical Engineering Journal* 2021;426:130345.
30 <https://doi.org/10.1016/j.cej.2021.130345>.
31
32 [83] Zeyrek Ongun M, Oguzlar S, Kartal U, Yurddaskal M, Cihanbegendi O. Energy harvesting
33 nanogenerators: Electrospun β -PVDF nanofibers accompanying ZnO NPs and ZnO@Ag
34 NPs. *Solid State Sci* 2021;122:106772.
35 <https://doi.org/10.1016/j.solidstatesciences.2021.106772>.
36
37 [84] Deng W, Yang T, Jin L, Yan C, Huang H, Chu X, et al. Cowpea-structured PVDF/ZnO
38 nanofibers based flexible self-powered piezoelectric bending motion sensor towards
39 remote control of gestures. *Nano Energy* 2019;55:516–25.
40 <https://doi.org/10.1016/j.nanoen.2018.10.049>.
41
42 [85] Khalifa M, Peravali S, Varsha S, Anandhan S. Piezoelectric Energy Harvesting Using Flexible
43 Self-Poled Electroactive Nanofabrics Based on PVDF/ZnO-Decorated SWCNT
44 Nanocomposites. *Jom* 2022;74:3162–71. <https://doi.org/10.1007/s11837-022-05342-9>.
45
46 [86] Sabry RS, Hussein AD. Nanogenerator based on nanocomposites PVDF/ZnO with different
47 concentrations. *Mater Res Express* 2019;6. <https://doi.org/10.1088/2053-1591/ab4296>.
48
49 [87] Chandran AM, Varun S, Mural PKS. Flexible electroactive PVDF/ZnO nanocomposite with
50 high output power and current density. *Polym Eng Sci* 2021;61:1829–41.
51 <https://doi.org/10.1002/pen.25704>.
52
53
54
55
56
57
58
59
60

- 1
2
3 [88] Marmolejo-Tejada JM, De La Roche-Yepes J, Pérez-López CA, Taborda JAP, Ávila A,
4 Jaramillo-Botero A. Understanding the Origin of Enhanced Piezoelectric Response in PVDF
5 Matrices with Embedded ZnO Nanoparticles, from Polarizable Molecular Dynamics
6 Simulations. *J Chem Inf Model* 2021;61:4537–43.
7 <https://doi.org/10.1021/acs.jcim.1c00822>.
8
9
10 [89] Yi J, Song Y, Zhang S, Cao Z, Li C, Xiong C. Corona-Poled Porous Electrospun Films of
11 Gram-Scale Y-Doped ZnO and PVDF Composites for Piezoelectric Nanogenerators.
12 *Polymers (Basel)* 2022;14. <https://doi.org/10.3390/polym14183912>.
13
14 [90] Bairagi S, Shahid-ul-Islam, Kumar C, Babu A, Aliyana AK, Stylios G, et al. Wearable
15 nanocomposite textile-based piezoelectric and triboelectric nanogenerators: Progress and
16 perspectives. *Nano Energy* 2023;118:108962.
17 <https://doi.org/10.1016/j.nanoen.2023.108962>.
18
19 [91] Anja Lund, Christian Jonasson, Christer Johansson, Daniel Haagenen BH. Piezoelectric
20 Polymeric Bicomponent Fibers Produced by Melt Spinning. *J Appl Polym Sci*
21 2012;126:490–500. <https://doi.org/10.1002/app>.
22
23 [92] Nilsson E, Lund A, Jonasson C, Johansson C, Hagström B. Poling and characterization of
24 piezoelectric polymer fibers for use in textile sensors. *Sens Actuators A Phys*
25 2013;201:477–86. <https://doi.org/10.1016/j.sna.2013.08.011>.
26
27 [93] Hadimani RL, Bayramol DV, Sion N, Shah T, Qián L, Shi S, et al. Continuous production of
28 piezoelectric PVDF fibre for e-textile applications. *Smart Mater Struct* 2013;22:104757.
29 <https://doi.org/10.1088/0964-1726/22/7/075017>.
30
31 [94] Krajewski AS, Magniez K, Helmer RJN, Schrank V. Piezoelectric force response of novel 2d
32 textile based pvdf sensors. *IEEE Sens J* 2013;13:4743–8.
33 <https://doi.org/10.1109/JSEN.2013.2274151>.
34
35 [95] Tascan M, Nohut S. Effects of process parameters on the properties of wet-spun solid
36 PVDF fibers. *Textile Research Journal* 2014;84:2214–25.
37 <https://doi.org/10.1177/0040517514535869>.
38
39 [96] Ruihang Huang, Siyang Zhang, Wen Zhang XY. Progress of zinc oxide-based
40 nanocomposites in the textile industry. *IET Collaborative Intelligent Manufacturing*
41 2021;3:281–9.
42
43 [97] Khan A, Ali Abbasi M, Hussain M, Hussain Ibupoto Z, Wissting J, Nur O, et al. Piezoelectric
44 nanogenerator based on zinc oxide nanorods grown on textile cotton fabric. *Appl Phys*
45 *Lett* 2012;101. <https://doi.org/10.1063/1.4766921>.
46
47 [98] Tan Y, Yang K, Wang B, Li H, Wang L, Wang C. High-performance textile piezoelectric
48 pressure sensor with novel structural hierarchy based on ZnO nanorods array for
49 wearable application. *Nano Res* 2021;14:3969–76. [https://doi.org/10.1007/s12274-021-](https://doi.org/10.1007/s12274-021-3322-2)
50 [3322-2](https://doi.org/10.1007/s12274-021-3322-2).
51
52
53
54
55
56
57
58
59
60

- 1
2
3 [99] Zhang Z, Chen Y, Guo J. ZnO nanorods patterned-textile using a novel hydrothermal
4 method for sandwich structured-piezoelectric nanogenerator for human energy
5 harvesting. *Physica E Low Dimens Syst Nanostruct* 2019;105:212–8.
6 <https://doi.org/10.1016/j.physe.2018.09.007>.
7
8
9 [100] Feng W, Chen Y, Wang W, Yu D. A waterproof and breathable textile pressure sensor with
10 high sensitivity based on PVDF/ZnO hierarchical structure. *Colloids Surf A Physicochem*
11 *Eng Asp* 2022;633:127890. <https://doi.org/10.1016/j.colsurfa.2021.127890>.
12
13 [101] Ojha DP, Joshi B, Samuel E, Khadka A, Aldalbahi A, Periyasami G, et al. Supersonically
14 Sprayed Flexible ZnO/PVDF Composite Films with Enhanced Piezoelectricity for Energy
15 Harvesting and Storage. *Int J Energy Res* 2023;2023:1–15.
16 <https://doi.org/10.1155/2023/3074782>.
17
18 [102] Islam MJ, Lee H, Lee K, Cho C, Kim B. Piezoelectric Nanogenerators Fabricated Using Spin
19 Coating of Poly(vinylidene fluoride) and ZnO Composite. *Nanomaterials* 2023;13.
20 <https://doi.org/10.3390/nano13071289>.
21
22 [103] Li Y, Sun J, Li P, Li X, Tan J, Zhang H, et al. High-performance piezoelectric nanogenerators
23 based on hierarchical ZnO@CF/PVDF composite film for self-powered meteorological
24 sensor. *J Mater Chem A Mater* 2023;11:13708–19. <https://doi.org/10.1039/d3ta01886e>.
25
26 [104] Jin C, Hao N, Xu Z, Trase I, Nie Y, Dong L, et al. Flexible piezoelectric nanogenerators using
27 metal-doped ZnO-PVDF films. *Sens Actuators A Phys* 2020;305:111912.
28 <https://doi.org/10.1016/j.sna.2020.111912>.
29
30 [105] Hari MA, Karumuthil SC, Varghese S, Rajan L. Performance Enhancement of Flexible and
31 Self-Powered PVDF-ZnO Based Tactile Sensors. *IEEE Sens J* 2022;22:9336–43.
32 <https://doi.org/10.1109/JSEN.2022.3166706>.
33
34 [106] Ojha DP, Joshi B, Samuel E, Khadka A, Aldalbahi A, Periyasami G, et al. Supersonically
35 Sprayed Flexible ZnO/PVDF Composite Films with Enhanced Piezoelectricity for Energy
36 Harvesting and Storage. *Int J Energy Res* 2023;2023:1–15.
37 <https://doi.org/10.1155/2023/3074782>.
38
39 [107] Islam MJ, Lee H, Lee K, Cho C, Kim B. Piezoelectric Nanogenerators Fabricated Using Spin
40 Coating of Poly(vinylidene fluoride) and ZnO Composite. *Nanomaterials* 2023;13.
41 <https://doi.org/10.3390/nano13071289>.
42
43 [108] Jin C, Hao N, Xu Z, Trase I, Nie Y, Dong L, et al. Flexible piezoelectric nanogenerators using
44 metal-doped ZnO-PVDF films. *Sens Actuators A Phys* 2020;305:111912.
45 <https://doi.org/10.1016/j.sna.2020.111912>.
46
47 [109] Pratihar S, Medda SK, Sen S, Devi PS. Tailored piezoelectric performance of self-polarized
48 PVDF-ZnO composites by optimization of aspect ratio of ZnO nanorods. *Polym Compos*
49 2020;41:3351–63. <https://doi.org/10.1002/pc.25624>.
50
51
52
53
54
55
56
57
58
59
60

- 1
2
3 [110] Iqbal T, Haq KU, Irfan M, Khalil M, Ramay SM, Ebdah MA, et al. Structural and optical
4 investigations on ZnO-PVDF-NiO advanced polymer composites for modern electronic
5 devices. *Mater Res Express* 2023;10. <https://doi.org/10.1088/2053-1591/acc92b>.
6
7 [111] Faruk Ünsal Ö, Bedeloğlu AÇ elik. Three-Dimensional Piezoelectric-Triboelectric Hybrid
8 Nanogenerators for Mechanical Energy Harvesting. *ACS Appl Nano Mater* 2023;6:14656–
9 68. <https://doi.org/10.1021/acsanm.3c01973>.
10
11 [112] Pu X, Zha JW, Zhao CL, Gong SB, Gao JF, Li RKY. Flexible PVDF/nylon-11 electrospun
12 fibrous membranes with aligned ZnO nanowires as potential triboelectric nanogenerators.
13 *Chemical Engineering Journal* 2020;398:125526.
14 <https://doi.org/10.1016/j.cej.2020.125526>.
15
16 [113] Singh HH, Khare N. Improved performance of ferroelectric nanocomposite flexible film
17 based triboelectric nanogenerator by controlling surface morphology, polarizability, and
18 hydrophobicity. *Energy* 2019;178:765–71. <https://doi.org/10.1016/j.energy.2019.04.150>.
19
20 [114] Aliyana AK, Naveen Kumar SK, Marimuthu P, Baburaj A, Adetunji M, Frederick T, et al.
21 Machine learning-assisted ammonium detection using zinc oxide/multi-walled carbon
22 nanotube composite based impedance sensors. *Sci Rep* 2021;11.
23 <https://doi.org/10.1038/s41598-021-03674-1>.
24
25 [115] Thakur VN, Han JI. Combined Triboelectric and Piezoelectric Effect in ZnO/PVDF Hybrid-
26 Based Fiber-Structured Nanogenerator with PDMS:Carbon Black Electrodes. *Polymers*
27 (Basel) 2022;14. <https://doi.org/10.3390/polym14204414>.
28
29 [116] Choi M, Murillo G, Hwang S, Woong Kim J, Hoon Jung J, Chen C-Y, et al. Mechanical and
30 Electrical Characterization of PVDF-ZnO Hybrid Structure for Application to
31 Nanogenerator. 2017.
32
33 [117] Narasimulu AA, Zhao P, Soin N, Prashanthi K, Ding P, Chen J, et al. Significant triboelectric
34 enhancement using interfacial piezoelectric ZnO nanosheet layer. *Nano Energy*
35 2017;40:471–80. <https://doi.org/10.1016/j.nanoen.2017.08.053>.
36
37 [118] Zheng Y, Cheng L, Yuan M, Wang Z, Zhang L, Qin Y, et al. Electrospun nanowire-based
38 triboelectric nanogenerator and its application on the full self-powered UV detector
39 Received (in XXX, XXX) Xth XXXXXXXXX 20XX, Accepted Xth XXXXXXXXX 20XX n.d.
40 <https://doi.org/10.1039/c0xx00000x>.
41
42 [119] Singh HH, Khare N. Flexible ZnO-PVDF/PTFE based piezo-tribo hybrid nanogenerator.
43 *Nano Energy* 2018;51:216–22. <https://doi.org/10.1016/j.nanoen.2018.06.055>.
44
45 [120] Šutka A, Sherrell PC, Shepelin NA, Lapčinskis L, Mālnieks K, Ellis A V. Measuring
46 Piezoelectric Output—Fact or Friction? *Advanced Materials* 2020;32:1–9.
47 <https://doi.org/10.1002/adma.202002979>.
48
49 [121] Bairagi S, Banerjee S, Chowdhury A, Ali SW. Development of a Sustainable and Flexible
50 Piezoelectric-cum-Triboelectric Energy Harvester Comprising a Simple Commodity Cotton
51
52
53
54
55
56
57
58
59
60

1
2
3 Fabric. ACS Sustain Chem Eng 2021;9:4004–13.
4 <https://doi.org/10.1021/acssuschemeng.0c07274>.

6 [122] Suo G, Yu Y, Zhang Z, Wang S, Zhao P, Li J, et al. Piezoelectric and Triboelectric Dual Effects
7 in Mechanical-Energy Harvesting Using BaTiO₃/Polydimethylsiloxane Composite Film. ACS
8 Appl Mater Interfaces 2016;8:34335–41. <https://doi.org/10.1021/acsami.6b11108>.

10 [123] Chen C, Zhao S, Pan C, Zi Y, Wang F, Yang C, et al. A method for quantitatively separating
11 the piezoelectric component from the as-received “Piezoelectric” signal. Nat Commun
12 2022;13:1–9. <https://doi.org/10.1038/s41467-022-29087-w>.
13
14
15
16
17
18
19
20
21
22
23
24
25
26
27
28
29
30
31
32
33
34
35
36
37
38
39
40
41
42
43
44
45
46
47
48
49
50
51
52
53
54
55
56
57
58
59
60